Title

Total-Body PET Imaging of Musculoskeletal Disorders

Journal

PET Clinics, 16(1)

ISSN

1556-8598

Authors

Chaudhari, Abhijit J

Raynor, William Y

Gholamrezanezhad, Ali

et al.

Publication Date

2021

DOI

10.1016/j.cpet.2020.09.012

Peer reviewed

HHS Public Access

Author manuscript

PET Clin. Author manuscript; available in PMC 2022 January 01.

Published in final edited form as:

PET Clin. 2021 January ; 16(1): 99–117. doi:10.1016/j.cpet.2020.09.012.

Total-Body PET Imaging of Musculoskeletal Disorders

Abhijit J. Chaudhari, PhD[1,*], **William Y. Raynor, BS**[2,3,*], **Ali Gholamrezanezhad, MD**[4], **Thomas J. Werner, MSE**[2], **Chamith S. Rajapakse, PhD**[2], **Abass Alavi, MD, MD (Hon), PhD (Hon), DSc (Hon)**[2]

[1]Department of Radiology, University of California Davis, 4860 Y Street, Sacramento, CA 95825, USA

[2]Department of Radiology, University of Pennsylvania, 3400 Spruce Street, Philadelphia, PA 19104, USA

[3]Drexel University College of Medicine, 2900 W Queen Lane, Philadelphia, PA 19129, USA

[4]Keck School of Medicine, University of Southern California, 1520 San Pablo Street, Los Angeles, CA 90033, USA.

Keywords

musculoskeletal disorders; arthritis; fever of unknown origin; osteoporosis; sarcopenia; cancer; osteosarcoma; PET; PET/CT; PET/MRI

Introduction

Musculoskeletal disorders (MSDs) are broadly defined as diseases or injuries of the joints, bones, muscles, nerves, tendons, ligaments, supporting soft tissues, cartilage, and spinal discs, and comprise over 150 diagnoses.[1] Commonly encountered examples are arthritis (such as rheumatoid arthritis, systemic lupus erythematous, or osteoarthritis), osteoporosis/osteopenia, sarcopenia, infection, neoplasms, and neck and lower back pain. MSDs are a major cause of disability worldwide, second only to mental and substance use disorders,[2] and have a significant negative impact on global population health. They are prevalent across the lifespan and have an astronomical societal cost that comes in the form of limited mobility, dexterity and functional ability, persistent pain, inability to work, early retirement from work, inability to participate in societal roles, depression, and increased risk of developing other chronic disease conditions.[3]

Corresponding author: Abhijit J. Chaudhari, PhD (ajchaudhari@ucdavis.edu), Department of Radiology, University of California Davis, 4860 Y Street, Sacramento, CA 95825.

*These authors contributed equally to this work

Conflict of Interest:

The authors have declared no conflicts of interest.

Disclosure Statement: UC Davis has a revenue-sharing agreement with United Imaging Healthcare. The authors have no other matters to disclose.

Clinical evaluation of MSDs mostly relies on a combination of physical examination, serum biomarkers and pain- and health-assessment questionnaires. Outside of radiography, other imaging modalities have had a limited role in MSD evaluation. Anatomical imaging data from radiography, computed tomography (CT), and magnetic resonance imaging (MRI) have been shown to be only weakly correlated with clinical signs and disease pathogenesis or treatment response.[4] Therefore, precise image-based parameters that could allow assessment of the molecular and pathophysiologic processes that underlie the disease state and its progression over time could play a crucial role in the evaluation of MSDs. Molecular imaging with positron emission tomography (PET)/CT and PET/MRI has been employed for MSD evaluation, but only in a limited number of studies.[5] This has been a direct consequence of the associated high cumulative radiation dose, especially in the context of evaluating chronic MSDs, patient discomfort from the relatively long image acquisition time, and the inability to examine multiple body structures or systems that that are known to be affected by MSD. Furthermore, the limited spatial resolution of standard PET scanners is suboptimal for visualizing and quantifying disease activity in small joints or tissues, which appear to be a bellwether of pathology in several MSDs.

In this chapter we provide our perspective about the potential role of total-body PET/CT (TB PET/CT) in the management of patients with MSDs, with emphasis on autoimmune and degenerative arthritis, musculoskeletal infection, osseous disorders, sarcopenia, and musculoskeletal malignancies. Throughout this scientific communication, we elaborate on three major physical characteristics of TB PET/CT systems that are deemed crucial for successful evaluation of MSD disorders: (1) the long axial field-of-view, which enables imaging multiple organs and systems simultaneously during the same phases of radiotracer distribution and uptake; (2) high geometric sensitivity, which allows the reduction of the administered radiotracer dose significantly and the shortening of the image acquisition time; and (3) higher spatial resolution compared to standard PET systems, which is essential for detecting and quantifying disease process in the small musculoskeletal structures such as small joints, tendons, and soft tissue structures.

Rheumatoid and Psoriatic Arthritis

Rheumatoid arthritis (RA) and psoriatic arthritis (PsA) are two common autoimmune disorders that are systemic in nature and cause an inflammatory reaction, particularly in the joints. They are a major cause of disability and loss of function in the adult population worldwide. The underlying causes of these disorders are unknown, and the majority of patients have no family history of these serious musculoskeletal disabilities. While the prevalence of both conditions increases by age, juvenile idiopathic arthritis (JIA), formerly known as juvenile rheumatoid arthritis (JRA), is now recognized as an independent clinical entity in the broad class of autoimmune arthritis.

Joint inflammation is considered the hallmark of autoimmune arthritis, and tenosynovitis (inflammation of the synovium and the tendons) is commonly presented in both RA and PsA. The entity named enthesitis (inflammation of the entheses), which is unique to PsA, is considered the hallmark for early tissue damage. The existing treatment modalities include a vast number of established approaches and new therapeutics, such as tumor necrosis factor

inhibitors, that target joint inflammation[6,7] and broadly show successful modification of the disease course.[8–10] Clinical evaluation of RA and PsA (based on a physical exam performed by a rheumatologist and serum biomarkers) underestimates disease burden and has limited sensitivity and specificity in assessing response to therapeutic interventions.[11,12] Conventional radiographs, MRI, and ultrasound scanning, while useful for assessing structural consequences of these disorders, do not directly determine disease activity at the cellular level, which is essential for early detection and determining response to therapy.[13] By now it is well established that structural abnormalities are a late manifestation of the disease process. As such, discrepancy and discordance between structural imaging findings in the evaluation of inflammatory arthropathies are not uncommon.[14] Recent advancement in quantitative and semi-quantitative standard anatomical imaging, such as contrast-enhanced ultrasound,[15,16] quantitative MRI,[17] and dual-energy CT iodine maps[18] have been somewhat successful in the evaluation and staging of inflammatory arthropathies and their response to treatment. However, further studies are necessary to confirm their accuracy and practicality in this setting. PET/CT imaging with radiotracers such as ^{18}F-fluorodeoxyglucose (FDG) and ^{18}F-sodium fluoride (NaF) has been shown to be highly sensitive and accurate in examining MSDs, particularly those with significant inflammation (Figure 1).[13]

FDG-based PET/CT imaging has been frequently employed for assessing RA and PsA at various stages of the disease and monitoring response to treatment. [13,19–28] In one research study by Raynor et al., global synovial FDG activity was measured in 19 RA patients.[29] These investigators employed a thresholding algorithm (ROVER software, ABX GmbH, Radeberg, Germany) to delineate focal FDG uptake in the synovial joints in the hands, elbows, shoulders, knees, and feet. PET parameters reflecting volume and uptake values with and without partial volume correction were found to be significantly higher in RA patients compared to healthy control subjects and correlated significantly with clinical features such as CD reactive protein, erythrocyte sedimentation rate, and swollen joint count. In addition to the joints assessed by Raynor et al., FDG-PET/CT has been proposed to assess involvement of the hip and temporomandibular joint in patients with RA.[30,31] A study by Jonnakuti et al. used PET imaging with NaF, a tracer that portrays osteoblastic activity, to assess knee involvement in RA.[32] The authors noted that increased NaF uptake was associated with increased knee degeneration determined by Kellgren-Lawrence grading; therefore, they concluded that NaF-PET/CT may have clinical utility in assessing bone changes in RA. These studies emphasize the utility of TB PET/CT in facilitating the assessment of joints throughout the body, which are frequently involved in systemic disorders such as RA and PsA and can be effectively evaluated with this technology (Figures 2 **and** 3).

Several concerns have been raised about the role of PET/CT in the autoimmune arthritis population,[33] such as significant ionizing radiation exposure during the course of the disease and monitoring of treatment response, long scan times in a population that is functionally impaired, limited spatial resolution, which may be suboptimal for evaluating small joints such as those of the extremities that are affected early in the disease course, and examination of only a small anatomic segment of the body despite the clear need for systemic

assessment. As noted above, the unique characteristics of TB PET/CT including the long axial field-of-view, high sensitivity, and excellent spatial resolution could overcome the challenges that are faced with conventional PET instruments. Particularly, TB PET/CT would enable (i) staging of RA or PsA disease activity in the entire body, as opposed to examining only a limited subset of joints, so that the appropriate therapy for each individual patient and disease state can be adopted and therefore improving the outcome;[34,35] (ii) monitoring response to therapy in joint tissues to optimize the therapeutic window[36] and drug efficacy on a personalized basis,[37–39] switching promptly to another treatment in non-responders;[40,41] and (iii) assessing the influence of treatment on other crucial organ system, such as the cardiovascular system,[42] to reduce co-morbidities and side-effects.[43–45] In the juvenile population, the potential of lowering radiation dose and shortening scan time will also be of great importance since the incidence of autoimmune arthritis is relatively high in this age group.

Based on published literature, the majority of research studies in autoimmune arthritis have employed FDG as the main PET tracer. Molecular and cellular events that underlie the inflammatory-proliferative cascade in autoimmune arthritis include activation and transmigration of leucocytes, aberrant pathways of T-cell activation, angiogenesis, hypoxia, and increased osteoclastic and impaired osteoblastic activity and appear to play an important role in the pathogenesis of these disorders.[46–48] There are significant gaps in the knowledge regarding the exact role of these biological processes and their interactions during autoimmune arthritis pathogenesis. With the growing number of PET ligands,[49] these processes could be effectively examined by TB PET/CT to determine their role in these serious and yet treatable systemic inflammatory disorders. Such targeted research studies can also be of value in developing effective drugs in the future. While most PET imaging studies are performed as a single static scan at a late time point (mostly at 1-2 hours after the administration of the tracer), performing dynamic imaging with TB PET/CT may lead to improved knowledge in these conditions.[50,51]

In summary, employing TB PET/CT imaging will lead to a significantly lower radiation dose, shorter scan time, and optimal quantification of the disease burden of autoimmune arthritides such as RA and PsA. This could address significant obstacles and longstanding challenges that have been faced in the fields of rheumatology about staging disease activity, treatment options, long-term monitoring, and assessing treatment response.

Osteoarthritis and Degenerative Conditions

Osteoarthritis (OA) is a degenerative disease that is frequently associated with aging, obesity, and prior joint trauma or secondary to inflammatory arthropathies (such as RA and gout) or avascular necrosis.[52] This disorder represents one of the leading causes of impaired mobility in the elderly, and its prevalence is expected to increase as global life expectancy increases in the coming decades.[53] Although OA most commonly affects the spine, hip, knee, hands, and feet, it can potentially involve any synovial joint.[54] OA is characterized by systemic joint inflammation, exacerbated by proinflammatory changes that are related to aging as well as obesity,[55,56] and therefore this disease is an excellent candidate for imaging by PET/CT and PET/MRI.[57,58] In particular, FDG-PET/CT, as a validated and effective

method for detecting and quantifying synovitis due to OA, is ideally suited for assessing this very common joint disease.[57] Wandler et al. found that uptake of FDG in the shoulder was associated with OA, bursitis, frozen shoulder, and rotator cuff injury.[59] FDG uptake in the knee synovium of symptomatic OA patients has been found to be higher compared to that of control subjects.[60] In addition, FDG uptake in the knee has been associated with aging as well as clinical symptoms of OA unrelated to aging.[61,62]

In a recent study by Al-Zaghal et al., the role of FDG to assess degenerative changes in the knee was compared to that of NaF.[63] CT segmentation was used to quantify uptake of FDG, as an inflammatory biomarker, and NaF, as a tracer that reflects subchondral bone formation and turnover. Soft tissue FDG uptake was correlated with aging, and uptake of both tracers was correlated with patient body mass index. In a study of 34 subjects, Khaw et al. used NaF-PET/CT to evaluate bone turnover in the elbows, knees, hands, and feet.[64] PET segmentation using ROVER software facilitated the quantification of the volumetric and metabolic parameters of NaF-avid regions, which were used to determine global disease activity (Figure 4). Global PET parameters were found to correlate with subject body weight, suggesting that NaF-PET/CT is a sensitive method of determining the effects of biomechanical insufficiency on joint degeneration. To compare PET findings with those on MRI, Savic et al. used NaF-PET/MRI to evaluate changes related to OA in 16 patients with varying levels of disease.[65] The authors found that bone turnover determined by NaF-PET was correlated with degenerative changes in cartilage assessed by MRI. In two separate studies examining the hip joint, Kobayashi et al. demonstrated that NaF-PET can detect OA-related changes earlier than MRI and radiography and that NaF uptake correlated with pain severity.[66,67] Other studies have suggested that NaF uptake in the knee can identify changes before manifestation of abnormal findings on MRI.[68,69]

In addition to OA involving the appendicular skeleton, degenerative processes affecting the spine such as disc degeneration and spondylosis also cause inflammatory reactions and increased bone turnover that are detected as abnormal sites on PET. In a study of 43 healthy subjects, FDG uptake in the thoracic and lumbar spine was found to correlate with body weight, likely representing early inflammatory changes related to degeneration.[70] A similar study demonstrated an association between body weight and increased NaF uptake in the cervical, thoracic, and lumbar spine.[71] Rosen et al., who analyzed FDG-PET/CT images from 150 subjects, found that degenerative disk and facet disease present on CT correlated with FDG uptake.[72] PET imaging can also be used to diagnosis of other sources of back and neck pain that often cannot be visualized by other modalities and include radiculopathy, spondylitis, spondylodiscitis, and postsurgical complications and infections.[73–81] The findings from these studies suggest that PET has a potential role is assessing unknown causes of back pain in addition to detecting degenerative changes.

Since diseases affecting the skeleton can occur throughout the body, TB PET/CT is uniquely situated to diagnose and assess these common disorders. With the data available from TB PET/CT, future studies will be able to assess the total disease burden in the entire body rather than focusing on a subset of skeletal sites. FDG and NaF have been demonstrated to be feasible markers of degenerative processes, and global assessment of uptake of these tracers may have a future role in the determination of disease severity and response to

therapy. PET tracers beyond FDG and NaF that target other pathologic processes involved in joint degeneration, such as angiogenesis or macrophage activity, potentially may reveal novel therapeutic targets.

Fever of Unknown Origin

The classic definition of fever of unknown origin (FUO) was first described in 1961 by Petersdorf and Beeson, who defined it as: “fever higher than 38.3°C (100.9°F) on several occasions, persisting without diagnosis for at least 3 weeks in spite of at least 1 week’s investigation in hospital.”[82,83] The definition of FUO was later revised and now includes cases in which three outpatient visits have not resulted in a diagnosis.[84] Causes of FUO include infection, inflammatory diseases, and malignancy, with more than 200 differential diagnoses being recognized.[84–86] Musculoskeletal infections are an important cause of FUO. Although conventional modalities, such as radiography, ultrasound, CT, and MRI are typically first-line options, by definition, in a majority of these cases no known musculoskeletal source of infection can be suspected and imaged specifically by these modalities. Therefore, a total-body imaging approach is of paramount importance and advantage in this setting. Moreover, equivocal findings on structural imaging modalities may warrant further evaluation with molecular modalities. In recent years, imaging with FDG-PET has become the study of choice in patients with FUO, which in the past was assessed by planar ^{67}Ga-citrate or ^{111}In-labelled white blood cell (^{111}In-WBC) scintigraphy.[84] In a prospective study that compared FDG-PET and ^{67}Ga-citrate imaging in 58 patients, FDG-PET successfully detected the source FUO in 35% of cases, while ^{67}Ga-citrate was helpful in 25% of the subjects examined.[87] Since all ^{67}Ga-citrate positive cases were also visualized by FDG-PET, the authors concluded that the latter could replace other techniques for this purpose. A prospective study of 23 patients found that FDG-PET had a sensitivity and specificity of 86% and 78% in determining the etiology of FUO, compared to 20% and 100% by ^{111}In-WBC scintigraphy.[88] A meta-analysis comparing the utility of FDG-PET/CT, FDG-PET, ^{67}Ga-citrate, and ^{111}In-WBC scintigraphy in evaluating FUO found that FDG-PET/CT had the highest sensitivity of 86% and the highest diagnostic yield of 58%.[89]

Among applications of FDG-PET/CT for the assessment of bone and soft-tissue infections, that of diabetic foot has been studied the most over the past two decades.[90–96] The possibility of diabetic neuropathy resulting in neuropathic osteoarthropathy makes diagnosis of osteomyelitis in this setting difficult by traditional clinical and radiographic techniques.[93,97] In addition to its utility in assessing FUO with suspected osteomyelitis, FDG-PET/CT has also been shown to be able to differentiate osteomyelitis from neuropathic osteoarthropathy and soft-tissue infections.[90–94,96] Besides FDG, other tracers such as NaF, ^{11}C-methionine, ^{68}Ga-citrate, ^{11}C-PK11195, and ^{124}I-FIAU have been used with PET imaging to detect and characterize osteomyelitis.[97,98] Alternatively, PET imaging with FDG-labeled autologous leukocytes has been reported to have a sensitivity of 83.3% and specificity of 100% in the diagnosis of osteomyelitis of the foot in patients with diabetes.[99,100] However, the role of the latter approach is very questionable and should not be considered for future clinical and research activities.

With increased validation for PET in the diagnosis of musculoskeletal infections and other differential causes of FUO, it becomes imperative that TB PET/CT be utilized in this domain. The nature of FUO often indicates that the underlying cause cannot be detected and localized by conventional means, and therefore only imaging of the entire body would be ideally suited to examine patients with this diagnosis. Although FDG will play a critical role in the setting of musculoskeletal infections, other PET tracers have shown some promise[49] and may also benefit from the unique capabilities of TB PET/CT.

Osteopenia and Osteoporosis

Osteoporosis, a disease characterized by increased osseous fragility and risk of fracture, has reached epidemic proportions. It affects 10 million Americans, resulting in two million fragility fractures per year.[101] Osteoporosis is known to be a systemic disease, and age-related bone fractures could happen in any part of the skeleton. Vertebral fractures are the most common fragility fractures. Of all the osteoporotic fractures, hip fractures have the most devastating[102103] consequences. The mortality rate in the year following a hip fracture is as high as 30%. Less than half of patients who had a hip fracture regain their previous level of function.[103,104] Other skeletal sites for fragility fractures include the wrist, pelvis, humerus, ankle, and foot.

The current standard-of-care test for the assessment of metabolic bone diseases, including osteoporosis, involves the use of dual energy X-ray absorptiometry (DXA).[105] DXA provides a measure of areal bone mineral density (BMD) at the hip or lumbar spine. Severity of the disease is typically quantified by the BMD T-score, which represents the standard deviations above or below the mean of a young healthy population. According to the World Health Organization (WHO) a T-score between −1.0 and −2.5 is defined as osteopenia and less than −2.5, osteoporosis.[106,107] DXA-derived BMD, a surrogate for bone quality, has many limitations, including the two-dimensional nature and poor image quality. Also, the evaluation of BMD by DXA can be confounded by osteophytosis, resulting in erroneously high quantitative values.[108] As a consequence, over 50% of women who sustain a hip fracture have BMD T-scores > −2.5, i.e., above the threshold for osteoporosis diagnosis and treatment.[109] Three-dimensional imaging modalities such as MRI[110,111] and CT[112–114] have been shown to have better performance in assessing metabolic bone diseases, particularly the bone strength, compared to DXA. However, the above mentioned imaging modalities provide only structural information about bone. Since bone is a slow-changing organ at the macro and micro level, structural changes induced by age or disease or in response to therapy cannot be detected using conventional bone imaging modalities until several months to years have passed.

Limitations in current bone imaging modalities have resulted in the exploration of novel methodologies for better assessment of bone quality. In recent years, NaF-PET/CT has emerged as a modality that can quantify changes in bone health and integrity, including in benign conditions.[115–117] Affinity of NaF to bone involves the diffusion of the radiotracer through capillaries into the extracellular fluid of the bone and the exchange of the fluoride ion with a hydroxyl group in the hydroxyapatite mineral on bone surfaces during

remodeling.[118] As a result, NaF uptake can be used as a measure of osteoblast activity and hence, bone turnover.

Quantification of both bone plasma clearance and bone uptake of NaF has been employed in the assessment of bone turnover. Both the Hawkins method and the Patlak Plot method are available to determine bone plasma clearance and require dynamic imaging. Alternatively, uptake is easily determined by a static scan and is often expressed as a standardized uptake value (SUV), which represents measured activity normalized to body weight and administered dose of tracer.[119] NaF uptake at the femoral neck was found to decrease with age and correlated with CT-derived BMD in a study that included 68 female subjects and 71 male subjects.[120] A study of 72 postmenopausal women classified as normal, osteopenic, or osteoporotic determined by DXA demonstrated decreased lumbar spine plasma clearance of NaF in osteoporotic subjects compared to both normal and osteopenic subjects.[121] Another study using NaF uptake showed similar findings of decreased bone turnover at the lumbar spine in patients diagnosed with osteoporosis compared to patients with a T score above −2.5.[122] Besides osteoporosis, NaF-PET/CT has also shown utility in assessing metabolic bone diseases,including Paget disease of bone.[123,124]

Evaluating the effects of treatment for osteoporosis is a major potential application of NaF-PET/CT. Antiresorptive therapy with bisphosphonates such as alendronate and risedronate is known to rapidly decrease bone resorption, followed by a decrease in bone formation. Accordingly, treatment of 18 women with risedronate resulted in an 18% decrease in lumbar spine plasma clearance of NaF after six months.[125] Similarly, in a study of 24 postmenopausal women with glucocorticoid-induced osteoporosis treated with alendronate, NaF uptake decreased by 14% in the lumbar spine and by 24% in the femoral neck after 12 months.[122] Frost et al. assessed changes after discontinuation of alendronate and risedronate on NaF uptake in the spine, hip, and femur of 20 postmenopausal women.[126] The authors found that although bone turnover in the spine remained suppressed, uptake in the hip and femur increased after 12 months in patients who had taken alendronate. Treatment with teriparatide results in an increase in both bone resorption and bone formation. In 18 postmenopausal women treated with teriparatide for six months, plasma clearance of NaF at the spine as well as uptake at the femoral shaft and pelvis were observed to increase significantly.[127]

In addition to the spine, pelvis, and femur, NaF-PET/CT has also been used to assess bone formation at the parietal bone, humerus, sternum, and tibia.[128,129] The calcaneus is a bone that presents with increased fracture risk due to osteoporosis. Although there have been several studies using MRI to assess calcaneal involvement in osteoporosis,[130,131] no studies have used NaF-PET/CT yet for this purpose. TB PET/CT would ensure that all areas of concern such as the calcaneus can be assessed for low bone turnover and therefore risk for fragility fracture. Using CT segmentation, metabolic activity in the whole skeleton can be quantified on PET (Figure 5). Zirakchian Zadeh et al. used this methodology to measure NaF uptake in the whole skeleton of multiple myeloma patients to assess changes in bone turnover after therapy.[132] A similar methodology could be applied to TB PET/CT images to determine systemic bone turnover in the entire skeleton in addition to the assessment of individual bones.

Due to scan time and radiation dose restrictions, conventional bone imaging modalities typically focus on one anatomic site for the assessment of metabolic bone diseases. Although osteoporosis and osteopenia are known to be systemic in nature bone quality at one skeletal site does not reflect the bone health at another site.[133] It is also known that bone metabolism is skeletal site dependent.[134] It is therefore useful to have the capability to assess the bone quality at all skeletal sites that are susceptible to osteoporotic fracture. TB PET/CT provides a unique opportunity to assess bone metabolism in the entire skeleton in one scan, and in the same phase of radiotracer distribution and uptake. In short, faster scan time, lower dose, and entire body coverage achievable by TB PET/CT could enable earlier detection of metabolic bone diseases before structural changes in bone could be detected by other imaging modalities.

Skeletal Muscle

The human body consists of over 500 skeletal muscles primarily responsible for contraction and relaxation and supporting other tissues of the skeletal system.[135] Skeletal muscles are distributed across the entire body, and play a crucial role in physical performance, glucose homeostasis and other metabolic functions.[136,137] Therefore, skeletal muscle loss or dysfunction can have severe health consequences, ranging from functional disability and institutionalization[138] to insulin resistance, metabolic syndrome, and obesity.[139] Sarcopenia, broadly defined as clinically significant loss of muscle mass and function, is now recognized as a hallmark of ageing.[140] Besides ageing, sarcopenia can also occur in other conditions such as autoimmune arthritis, heart failure, and cancer (commonly referred to as cachexia).[141] Sarcopenia presence increases both risk for hospitalization and cost of care during hospitalization,[142] with a two-fold or more increase in overall cost compared to those without the condition.[143] Sarcopenia is recognized as a muscle disease with an ICD-10-CM code that can be used to bill for care in some countries.[144]

To date, anatomical imaging methods, such as DXA, CT, MRI, and ultrasound have been used to assess surrogate measures of muscle mass and quality of relevance to sarcopenia.[140,145] While muscle mass can be reliability estimated using these methods (via detailed image segmentation), there is no consensus on the metrics of muscle quality that best represent prognostic value.[146] For example, the degree of fat infiltration in muscle changes the latter's Hounsfield unit (HU) value in CT images and may provide an assessment of muscle quality; however, there is no standardization regarding CT thresholds to establish sarcopenia diagnosis across the different conditions.[146,147] Furthermore, these anatomical imaging modalities are unable to assess the molecular activity of skeletal muscle. On the other hand, PET has been shown to be sensitive to muscle blood flow, protein synthesis, and glucose metabolism, and has been utilized in the assessment of skeletal muscle with applications ranging from diabetes[148] and cancer-related dysfunction,[149,150] to exercise physiology.[151,152] Studies suggest that PET may provide information regarding skeletal muscle quality that is unattainable from structural imaging modalities.[149,153] Commonly used PET radiotracers in the published literature to evaluate skeletal muscle are ^{15}O-water,[154–156] ^{11}C-methyl-methionine[157] and FDG.[158–160] A number of other radiotracers targeting key pathological processes underlying sarcopenia are under development or are being explored in early-stage human studies.[161–163]

Currently, PET/CT has a limited role in the clinical assessment of sarcopenia. However, TB PET/CT could overcome shortcomings of the existing methods. First, sarcopenia is not limited to just a few muscles,[164,165] meaning that no single muscle or muscle group is a robust representative of the systemic burden of sarcopenia.[166] TB PET/CT enables the assessment of the entire skeletal muscle in the body in the same phases of radiotracer distribution and uptake, and can therefore contribute towards a more comprehensive and global analysis of sarcopenia (Figure 6). Second, TB PET/CT could play a critical role in the longitudinal monitoring of sarcopenia, as the cumulative doses will be significantly lower and image acquisition is relatively fast. Third, the combination of higher spatial resolution and geometric sensitivity of TB PET/CT compared to current scanners will enable delineating activity of the different muscle groups to better understand sarcopenia pathogenesis,[167] and heterogeneity of radiotracer uptake,[152,168] which may provide insights for intervention. Lastly, TB PET/CT measures are quantitative and therefore provide reliable and reproducible data compared with those from physical examination and structural imaging.

In summary TB PET/CT measures may usher in several new biomarkers of sarcopenia that will be helpful both for understanding the underlying pathogenesis of the condition and for the evaluation of and monitoring of interventions and therapy.

Neoplastic Musculoskeletal Diseases

Bone and soft tissue cancers of the musculoskeletal system are relatively uncommon but have significant impact on quality of life and are commonly associated with high morbidity and mortality in the affected population. These malignancies commonly metastasize to distant organs which may not be successfully detected and monitored by conventional imaging techniques. Whole-body PET in this setting has the advantage of imaging both the primary lesion and the metastatic sites with a single image acquisition procedure.[169–171] Hybrid imaging with PET/MRI provides certain advantages over PET/CT, as PET/MRI allows higher reading confidence compared to PET/CT.

Most malignant tumors of the musculoskeletal system demonstrate increased FDG uptake due to their high glycolytic activity compared to the surrounding normal tissue structures. FDG-PET not only allows differentiation of soft tissue and osseous lesions that cannot be fully defined by structural imaging modalities alone, but is also a key component for staging/restaging of the disease and treatment planning (Figure 7).[171–173] Erfanian et al. reported a higher accuracy for PET/MRI compared to MRI alone in delineating soft tissue malignancies.[172] In a recent study by Cleary et al., who examined patients with osteosarcoma, 81% were noted to have suspicious popliteal lymph nodes on the initial MRI. However, in contrast to MRI, only one node was presumed to be metastatic based on its increased metabolic activity on PET/CT, a finding that was further confirmed in the 12 months follow-up assessment.[171]

PET is commonly employed for follow-up of aggressive bone and soft tissue tumors to evaluate therapy response and is often superior to structural imaging alone for this purpose. In fact, molecular imaging is the mainstay of personalized therapeutic approaches in

musculoskeletal cancer treatment. A recent study reported by Lee et al. described the impact of PET/CT in managing 73 patients with stage II osteosarcomas of the extremities who were treated with two cycles of neoadjuvant chemotherapy, surgical resection, and adjuvant chemotherapy. These patients underwent PET/CT before treatment (PET0), after 1 cycle of chemotherapy (PET1), and following the completion of neoadjuvant chemotherapy (PET2). They noted that evidence for response to treatment after the first cycle of preoperative chemotherapy was best predicted by PET.[174] This research demonstrated that PET was a powerful modality for early response monitoring by providing the opportunity of early modification of timing of local control. SUV_{max} on PET2, the delta (percentage change) of SUV_{max} between PET0 and PET1, and between PET0 and PET2 have been proposed by these researchers as the most accurate predictors of poor response and development of future metastatic events. Based on the data generated, patients with SUV of more than 5.9 on PET2 had a poor event-free survival compared to the others.[174] The features provided by PET have been further augmented by the incorporation of artificial intelligence, texture analysis, and machine learning into image interpretation.[175,176]

Despite all the advantages associated with this modality, some studies have warned about false negative results with PET imaging. A retrospective study on 24 histopathologically confirmed cases of Ewing sarcoma who underwent MRI and FDG-PET/CT within a 4-week interval demonstrated that some of the osseous metastases detected by MRI may not show increased metabolic activity on FDG-PET/CT, rendering them as false-negative results.[177] Therefore, it has been advised that caution should be exercised in interpreting FDG-PET/CT for the detection of skeletal metastases in Ewing sarcoma. Likely, the potential source of such false negative results is due to the presence of low contrast resolution between bone metastases and the background hematopoietic marrow, hematopoietic reconversion due to recent chemotherapy, and/or due to the small size of the lesions that are not detectable by PET. In contrast, MRI may not be significantly affected by these factors.[177] We believe these findings emphasize the importance of integrated PET/MRI in these settings by combining the advantages of molecular imaging with those of MRI by providing structural details.[5,178,179] Also, it has been widely accepted that non-contrast chest CT is the modality of choice for the evaluation of pulmonary metastases of osteosarcoma and Ewing sarcoma due to suboptimal sensitivity of PET/CT in detecting lung nodules that are smaller than 2 cm and are located in the lower lobes (due to technical limitations of respiratory motion gating and misregistration of PET and CT scans).[180–182] However, TB PET/CT imaging may overcome some of these shortcomings by acquiring images over a shorter period of time and at later time points (at 3-4 hours).

Discussion

As PET-based techniques become increasingly validated, their application to MSDs, such as arthritis, infection, osteoporosis, sarcopenia, and soft tissue and osseous neoplastic pathologies, will continue to grow. Many of these disorders are difficult to diagnose, stage, and evaluate over time with conventional imaging modalities. FDG and NaF among other tracers have the potential to reveal molecular processes before evidence of disease is present clinically or structurally on conventional imaging techniques. Although reported studies in the literature are based on examining individual joints, bones, and muscles, TB PET/CT will

allow for a comprehensive and systematic evaluation of the MSDs that cannot easily be localized to one specific region. The introduction of TB PET/CT in this domain may allow for improved detection of many abnormalities throughout the body, accurate monitoring, and a better understanding of the effects of the current and future therapeutic intervention.

However, before TB PET/CT can be widely adopted, certain aspects of this modality require further consideration and optimization. Regarding chronic conditions as well as pediatric applications, ionizing radiation dose may be a concern, and a cost-to-benefit analysis would be warranted to determine optimal scan frequency. Furthermore, depending on the kinetics of the radiotracer, the preferred scanning start time and duration may be disease-specific, causing difficulty in visualizing unrelated findings (such as evaluating cardiovascular disease in RA). Lastly, reconstruction parameters will also depend on the structure of interest. For example, imaging of small joints in RA would warrant parameters that produce high resolution, but high variance, while imaging of large muscles would warrant parameters that produce low variance, but lower resolution. Future research regarding the tradeoffs involved in each of these considerations would support the efficient use of TB PET/CT and facilitate wider applications of this new but very promising technology.

Acknowledgements:

The authors would like to acknowledge support by the National Institutes of Health under award number R01AR076088.

References

1. Briggs AM, Cross MJ, Hoy DG, et al. Musculoskeletal Health Conditions Represent a Global Threat to Healthy Aging: A Report for the 2015 World Health Organization World Report on Ageing and Health. Gerontologist. 2016;56 Suppl 2:S243–255. [PubMed: 26994264]
2. Murray CJ, Barber RM, Foreman KJ, et al. Global, regional, and national disability-adjusted life years (DALYs) for 306 diseases and injuries and healthy life expectancy (HALE) for 188 countries, 1990–2013: quantifying the epidemiological transition. The Lancet. 2015;386(10009):2145–2191.
3. March L, Smith EU, Hoy DG, et al. Burden of disability due to musculoskeletal (MSK) disorders. Best Practice & Research: Clinical Rheumatology. 2014;28(3):353–366. [PubMed: 25481420]
4. Put S, Westhovens R, Lahoutte T, Matthys P. Molecular imaging of rheumatoid arthritis: emerging markers, tools, and techniques. Arthritis research & therapy. 2014;16(2):208. [PubMed: 25099015]
5. Gholamrezanezhad A, Guermazi A, Salavati A, Alavi A. Evolving Role of PET-Computed Tomography and PET-MR Imaging in Assessment of Musculoskeletal Disorders and Its Potential Revolutionary Impact on Day-to-Day Practice of Related Disciplines. PET Clin. 2018;13(4):xiii–xiv.
6. Cheung TT, Mclnnes IB. Future therapeutic targets in rheumatoid arthritis? Paper presented at: Seminars in immunopathology 2017.
7. Tak PP. Analyzing synovial tissue samples. What can we learn about early rheumatoid arthritis, the heterogeneity of the disease, and the effects of treatment? J Rheumatol. 2005;32(Suppl 72):25–26.
8. Singh JA, Hossain A, Tanjong Ghogomu E, et al. Biologics or tofacitinib for people with rheumatoid arthritis unsuccessfully treated with biologics: a systematic review and network meta-analysis. Cochrane Database Syst Rev. 2017;3(3):CD012591. [PubMed: 28282491]
9. Singh JA, Saag KG, Bridges SL Jr SL, et al. 2015 American College of Rheumatology guideline for the treatment of rheumatoid arthritis. Arthritis & rheumatology. 2016;68(1):1–26.
10. Scott DL. Biologics-based therapy for the treatment of rheumatoid arthritis. Clin Pharmacol Ther. 2012;91(1):30–43. [PubMed: 22166850]

11. Forien M, Ottaviani S. Ultrasound and follow-up of rheumatoid arthritis. Joint Bone Spine. 2017;84(5):531–536. [PubMed: 27777169]
12. Kennish L, Labitigan M, Budoff S, et al. Utility of the new rheumatoid arthritis 2010 ACR/EULAR classification criteria in routine clinical care. BMJ Open. 2012;2(5):e001117.
13. Mountz JM, Alavi A, Mountz JD. Emerging optical and nuclear medicine imaging methods in rheumatoid arthritis. Nat Rev Rheumatol. 2012;8(12):719–728. [PubMed: 23007740]
14. Serban O, Fodor D, Papp I, et al. Reasons for discordances between ultrasonography and magnetic resonance imaging in the evaluation of the ankle, hindfoot and heel of the patients with rheumatoid arthritis. Med Ultrason. 2019;21(4):405–413. [PubMed: 31765448]
15. Liu H, Huang C, Chen S, et al. Value of contrast-enhanced ultrasound for detection of synovial vascularity in experimental rheumatoid arthritis: an exploratory study. J Int Med Res. 2019;47(11):5740–5751. [PubMed: 31547746]
16. Zhao C, Zhang R, Luo Y, et al. Multimodal VEGF-Targeted Contrast-Enhanced Ultrasound and Photoacoustic Imaging of Rats with Inflammatory Arthritis: Using Dye-VEGF-Antibody-Loaded Microbubbles. Ultrasound Med Biol. 2020.
17. Bennett JL, Wood A, Smith N, et al. Can quantitative MRI be used in the clinical setting to quantify the impact of intra-articular glucocorticoid injection on synovial disease activity in juvenile idiopathic arthritis? Pediatr Rheumatol Online J. 2019;17(1):74. [PubMed: 31752877]
18. Kayama R, Fukuda T, Ogiwara S, et al. Quantitative analysis of therapeutic response in psoriatic arthritis of digital joints with Dual-energy CT iodine maps. Sci Rep. 2020;10(1):1225. [PubMed: 31988331]
19. Fosse P, Kaiser MJ, Namur G, de Seny D, Malaise MG, Hustinx R. (18)F- FDG PET/CT joint assessment of early therapeutic response in rheumatoid arthritis patients treated with rituximab. European journal of hybrid imaging. 2018;2(1):6. [PubMed: 29782593]
20. Kubota K, Yamashita H, Mimori A. Clinical Value of FDG-PET/CT for the Evaluation of Rheumatic Diseases: Rheumatoid Arthritis, Polymyalgia Rheumatica, and Relapsing Polychondritis. Seminars in nuclear medicine. 2017;47(4):408–424. [PubMed: 28583280]
21. Raynor W, Houshmand S, Gholami S, et al. Evolving Role of Molecular Imaging with (18)F-Sodium Fluoride PET as a Biomarker for Calcium Metabolism. Curr Osteoporos Rep. 2016;14(4):115–125. [PubMed: 27301549]
22. Chaudhari AJ, Ferrero A, Godinez F, et al. High-resolution 18F-FDG PET/CT for assessing disease activity in rheumatoid and psoriatic arthritis: findings of a prospective pilot study. The British Journal of Radiology. 2016;89(1063):20160138. [PubMed: 27109738]
23. Yamashita H, Kubota K, Mimori A. Clinical value of whole-body PET/CT in patients with active rheumatic diseases. Arthritis research & therapy. 2014;16(5):423. [PubMed: 25606590]
24. Kubota K, Ito K, Morooka M, et al. FDG PET for rheumatoid arthritis: basic considerations and whole-body PET/CT. Annals of the New York Academy of Sciences. 2011;1228:29–38. [PubMed: 21718320]
25. Chaudhari AJ, Bowen SL, Burkett GW, et al. High-resolution (18)F-FDG PET with MRI for monitoring response to treatment in rheumatoid arthritis. Eur J Nucl Med Mol Imaging. 2010;37(5):1047. [PubMed: 20119695]
26. Beckers C, Ribbens C, Andre B, et al. Assessment of disease activity in rheumatoid arthritis with 18F-FDG PET. Journal of Nuclear Medicine. 2004;45(6):956–964. [PubMed: 15181130]
27. Yun M, Kim W, Adam LE, Alnafisi N, Herman C, Alavi A. F-18 FDG uptake in a patient with psoriatic arthritis: imaging correlation with patient symptoms. Clin Nucl Med. 2001 ;26(8):692–693. [PubMed: 11452176]
28. Polisson RP, Schoenberg OI, Fischman A, et al. Use of magnetic resonance imaging and positron emission tomography in the assessment of synovial volume and glucose metabolism in patients with rheumatoid arthritis. Arthritis Rheum. 1995;38(6):819–825. [PubMed: 7779126]
29. Raynor WY, Jonnakuti VS, Zirakchian Zadeh M, et al. Comparison of methods of quantifying global synovial metabolic activity with FDG-PET/CT in rheumatoid arthritis. Int J Rheum Dis. 2019;22(12):2191–2198. [PubMed: 31721461]

30. Mupparapu M, Oak S, Chang YC, Alavi A. Conventional and functional imaging in the evaluation of temporomandibular joint rheumatoid arthritis: a systematic review. Quintessence Int. 2019;50(9):742–753. [PubMed: 31482155]

31. Bhattarai A, Nakajima T, Sapkota S, et al. Diagnostic value of 18F-fluorodeoxyglucose uptake parameters to differentiate rheumatoid arthritis from other types of arthritis. Medicine (Baltimore). 2017;96(25):e7130. [PubMed: 28640086]

32. Jonnakuti VS, Raynor WY, Taratuta E, Werner TJ, Alavi A, Baker JF. A novel method to assess subchondral bone formation using [18F]NaF-PET in the evaluation of knee degeneration. Nucl Med Commun. 2018;39(5):451–456. [PubMed: 29505483]

33. Narayan N, Owen DR, Taylor PC. Advances in positron emission tomography for the imaging of rheumatoid arthritis. Rheumatology (Oxford). 2017;56(11):1837–1846. [PubMed: 28181650]

34. Bastida C, Ruíz V, Pascal M, Yagüe J, Sanmartí R, Soy D. Is there potential for therapeutic drug monitoring of biologic agents in rheumatoid arthritis? British journal of clinical pharmacology. 2017;83(5):962–975. [PubMed: 27990682]

35. Woodrick RS, Ruderman EM. Safety of biologic therapy in rheumatoid arthritis. Nat Rev Rheumatol. 2011;7(11):639–652. [PubMed: 21989284]

36. Van Nies J, Krabben A, Schoones J, Huizinga T, Kloppenburg M, Van Der Helm-Van Mil A. What is the evidence for the presence of a therapeutic window of opportunity in rheumatoid arthritis? A systematic literature review. Annals of the rheumatic diseases. 2014;73(5):861–870. [PubMed: 23572339]

37. Zeman MN, Scott PJ. Current imaging strategies in rheumatoid arthritis. Am J Nucl Med Mol Imaging. 2012;2(2):174–220. [PubMed: 23133812]

38. Keen HI, Emery P. How should we manage early rheumatoid arthritis? From imaging to intervention. Current opinion in rheumatology. 2005;17(3):280–285. [PubMed: 15838237]

39. Wunder A, Straub RH, Gay S, Funk J, Muller-Ladner U. Molecular imaging: novel tools in visualizing rheumatoid arthritis. Rheumatology (Oxford). 2005;44(11):1341–1349. [PubMed: 15972356]

40. Favalli EG, Sinigaglia L, Becciolini A, et al. Two-year persistence of golimumab as second-line biologic agent in rheumatoid arthritis as compared to other subcutaneous tumor necrosis factor inhibitors: real-life data from the LORHEN registry. International journal of rheumatic diseases. 2018;21(2):422–430. [PubMed: 29082659]

41. Emery P, Gottenberg JE, Rubbert-Roth A, et al. Rituximab versus an alternative TNF inhibitor in patients with rheumatoid arthritis who failed to respond to a single previous TNF inhibitor: SWITCH-RA, a global, observational, comparative effectiveness study. Ann Rheum Dis. 2015;74(6):979–984. [PubMed: 24442884]

42. Rose S, Sheth NH, Baker JF, et al. A comparison of vascular inflammation in psoriasis, rheumatoid arthritis, and healthy subjects by FDG-PET/CT: a pilot study. Am J Cardiovasc Dis. 2013;3(4):273–278. [PubMed: 24224139]

43. Humphreys J, Hyrich K, Symmons D. What is the impact of biologic therapies on common co-morbidities in patients with rheumatoid arthritis? Arthritis research & therapy. 2016;18(1):282. [PubMed: 27906042]

44. Richards JS, Dowell SM, Quinones ME, Kerr GS. How to use biologic agents in patients with rheumatoid arthritis who have comorbid disease. BMJ (Clinical research ed). 2015;351:h3658.

45. Lahiri M, Dixon WG. Risk of infection with biologic antirheumatic therapies in patients with rheumatoid arthritis. Best practice & research Clinical rheumatology. 2015;29(2):290–305. [PubMed: 26362745]

46. Veale DJ, Fearon U. The pathogenesis of psoriatic arthritis. Lancet. 2018;391(10136):2273–2284. [PubMed: 29893226]

47. Konisti S, Kiriakidis S, Paleolog EM. Hypoxia—a key regulator of angiogenesis and inflammation in rheumatoid arthritis. Nature Reviews Rheumatology. 2012;8(3):153. [PubMed: 22293762]

48. McInnes IB, Schett G. The pathogenesis of rheumatoid arthritis. N Engl J Med. 2011;365(23):2205–2219. [PubMed: 22150039]

49. Gholamrezanezhad A, Basques K, Batouli A, et al. Non-oncologic Applications of PET/CT and PET/MR in Musculoskeletal, Orthopedic, and Rheumatologic Imaging: General Considerations, Techniques, and Radiopharmaceuticals. J Nucl Med Technol. 2017.
50. Yaqub M, Verweij NJ, Pieplenbosch S, Boellaard R, Lammertsma AA, Van Der Laken CJ. Quantitative Assessment of Arthritis Activity in Rheumatoid Arthritis Patients Using [11C] DPA-713 Positron Emission Tomography. International Journal of Molecular Sciences. 2020;21(9):3137.
51. Kogan F, Broski SM, Yoon D, Gold GE. Applications of PET-MRI in musculoskeletal disease. JMagn Reson Imaging. 2018;48(1):27–47. [PubMed: 29969193]
52. Fransen M, Simic M, Harmer AR. Determinants of MSK health and disability: lifestyle determinants of symptomatic osteoarthritis. Best Pract Res Clin Rheumatol. 2014;28(3):435–460. [PubMed: 25481425]
53. Nguyen US, Zhang Y, Zhu Y, Niu J, Zhang B, Felson DT. Increasing prevalence of knee pain and symptomatic knee osteoarthritis: survey and cohort data. Ann Intern Med. 2011 ;155(11):725–732. [PubMed: 22147711]
54. O'Neill TW, McCabe PS, McBeth J. Update on the epidemiology, risk factors and disease outcomes of osteoarthritis. Best Pract Res Clin Rheumatol. 2018;32(2):312–326. [PubMed: 30527434]
55. Greene MA, Loeser RF. Aging-related inflammation in osteoarthritis. Osteoarthritis Cartilage. 2015;23(11):1966–1971. [PubMed: 26521742]
56. Berenbaum F, Eymard F, Houard X. Osteoarthritis, inflammation and obesity. Curr Opin Rheumatol. 2013;25(1): 114–118. [PubMed: 23090672]
57. Hayashi D, Roemer FW, Guermazi A. Imaging of osteoarthritis-recent research developments and future perspective. Br JRadiol. 2018;91(1085):20170349. [PubMed: 29271229]
58. Al-Zaghal A, Raynor W, Khosravi M, Guermazi A, Werner TJ, Alavi A. Applications of PET Imaging in the Evaluation of Musculoskeletal Diseases Among the Geriatric Population. Semin Nucl Med. 2018;48(6):525–534. [PubMed: 30322478]
59. Wandler E, Kramer EL, Sherman O, Babb J, Scarola J, Rafii M. Diffuse FDG shoulder uptake on PET is associated with clinical findings of osteoarthritis. AJR Am J Roentgenol. 2005;185(3):797–803. [PubMed: 16120937]
60. Parsons MA, Moghbel M, Saboury B, et al. Increased 18F-FDG uptake suggests synovial inflammatory reaction with osteoarthritis: preliminary in-vivo results in humans. Nucl Med Commun. 2015;36(12):1215–1219. [PubMed: 26367212]
61. Saboury B, Parsons MA, Moghbel M, et al. Quantification of aging effects upon global knee inflammation by 18F-FDG-PET. Nucl Med Commun. 2016;37(3):254–258. [PubMed: 26555103]
62. Hong YH, Kong EJ. (18F)Fluoro-deoxy-D-glucose uptake of knee joints in the aspect of age-related osteoarthritis: a case-control study. BMC Musculoskelet Disord. 2013;14:141. [PubMed: 23607872]
63. Al-Zaghal A, Yellanki DP, Ayubcha C, Werner TJ, Hoilund-Carlsen PF, Alavi A. CT-based tissue segmentation to assess knee joint inflammation and reactive bone formation assessed by (18)F-FDG and (18)F-NaF PET/CT: Effects of age and BMI. Hell J Nucl Med. 2018;21(2):102–107. [PubMed: 30006643]
64. Khaw TH, Raynor WY, Borja AJ, et al. Assessing the effects of body weight on subchondral bone formation with quantitative (18)F-sodium fluoride PET. Ann Nucl Med. 2020.
65. Savic D, Pedoia V, Seo Y, et al. Imaging Bone-Cartilage Interactions in Osteoarthritis Using [(18)F]-NaF PET-MRI. Mol Imaging. 2016;15:1–12. [PubMed: 28654417]
66. Kobayashi N, Inaba Y, Tateishi U, et al. Comparison of 18F-fluoride positron emission tomography and magnetic resonance imaging in evaluating early-stage osteoarthritis of the hip. Nucl Med Commun. 2015;36(1):84–89. [PubMed: 25230054]
67. Kobayashi N, Inaba Y, Tateishi U, et al. New application of 18F-fluoride PET for the detection of bone remodeling in early-stage osteoarthritis of the hip. Clin Nucl Med. 2013;38(10):e379–383. [PubMed: 23603593]

68. Kogan F, Fan AP, McWalter EJ, Oei EHG, Quon A, Gold GE. PET/MRI of metabolic activity in osteoarthritis: A feasibility study. JMagn Reson Imaging. 2017;45(6):1736–1745. [PubMed: 27796082]
69. Draper CE, Quon A, Fredericson M, et al. Comparison of MRI and (1)(8)F-NaF PET/CT in patients with patellofemoral pain. J Magn Reson Imaging. 2012;36(4):928–932. [PubMed: 22549985]
70. Ayubcha C, Zadeh MZ, Rajapakse CS, et al. Effects of age and weight on the metabolic activities of the cervical, thoracic and lumbar spines as measured by fluorine-18 fluorodeoxyglucose-positron emission tomography in healthy males. Hell J Nucl Med. 2018;21(1):2–6. [PubMed: 29550840]
71. Ayubcha C, Zirakchian Zadeh M, Stochkendahl MJ, et al. Quantitative evaluation of normal spinal osseous metabolism with 18F-NaF PET/CT. Nucl Med Commun. 2018;39(10):945–950. [PubMed: 30086077]
72. Rosen RS, Fayad L, Wahl RL. Increased 18F-FDG uptake in degenerative disease of the spine: Characterization with 18F-FDG PET/CT. J Nucl Med. 2006;47(8):1274–1280. [PubMed: 16883005]
73. Peters M, Willems P, Weijers R, et al. Pseudarthrosis after lumbar spinal fusion: the role of (1)(8)F-fluoride PET/CT. Eur J Nucl Med Mol Imaging. 2015;42(12):1891–1898. [PubMed: 26290422]
74. Seifen T, Rodrigues M, Rettenbacher L, et al. The value of (18)F-fluoride PET/CT in the assessment of screw loosening in patients after intervertebral fusion stabilization. Eur J Nucl Med Mol Imaging. 2015;42(2):272–277. [PubMed: 25223421]
75. Nakahara M, Ito M, Hattori N, et al. 18F-FDG-PET/CT better localizes active spinal infection than MRI for successful minimally invasive surgery. Acta Radiol. 2015;56(7):829–836. [PubMed: 25080515]
76. Inanami H, Oshima Y, Iwahori T, Takano Y, Koga H, Iwai H. Role of 18F-fluoro-D-deoxyglucose PET/CT in diagnosing surgical site infection after spine surgery with instrumentation. Spine (Phila Pa 1976). 2015;40(2):109–113. [PubMed: 25384054]
77. Byrnes TJ, Xie W, Al-Mukhailed O, et al. Evaluation of neck pain with (18)F-NaF PET/CT. Nucl Med Commun. 2014;35(3):298–302. [PubMed: 24257482]
78. Quon A, Dodd R, Iagaru A, et al. Initial investigation of (1)(8)F-NaF PET/CT for identification of vertebral sites amenable to surgical revision after spinal fusion surgery. Eur J Nucl Med Mol Imaging. 2012;39(11):1737–1744. [PubMed: 22895860]
79. Seifen T, Rettenbacher L, Thaler C, Holzmannhofer J, Mc Coy M, Pirich C. Prolonged back pain attributed to suspected spondylodiscitis. The value of (1)(8)F-FDG PET/CT imaging in the diagnostic work-up of patients. Nuklearmedizin. 2012;51(5):194–200. [PubMed: 22614880]
80. Gamie S, El-Maghraby T. The role of PET/CT in evaluation of Facet and Disc abnormalities in patients with low back pain using (18)F-Fluoride. Nucl Med Rev Cent East Eur. 2008;11(1):17–21. [PubMed: 19173183]
81. Gratz S, Dorner J, Fischer U, et al. 18F-FDG hybrid PET in patients with suspected spondylitis. Eur J Nucl Med Mol Imaging. 2002;29(4):516–524. [PubMed: 11914890]
82. Wright WF, Auwaerter PG. Fever and Fever of Unknown Origin: Review, Recent Advances, and Lingering Dogma. Open Forum Infect Dis. 2020;7(5):ofaa132. [PubMed: 32462043]
83. Petersdorf RG, Beeson PB. Fever of unexplained origin: report on 100 cases. Medicine (Baltimore). 1961;40:1–30. [PubMed: 13734791]
84. Hess S FDG-PET/CT in Fever of Unknown Origin, Bacteremia, and Febrile Neutropenia. PET Clin. 2020;15(2):175–185. [PubMed: 32145888]
85. Al-Zaghal A, Raynor WY, Seraj SM, Werner TJ, Alavi A. FDG-PET imaging to detect and characterize underlying causes of fever of unknown origin: an unavoidable path for the foreseeable future. Eur J Nucl Med Mol Imaging. 2019;46(1):2–7. [PubMed: 30242428]
86. Mulders-Manders C, Simon A, Bleeker-Rovers C. Fever of unknown origin. Clin Med (Lond). 2015;15(3):280–284. [PubMed: 26031980]
87. Blockmans D, Knockaert D, Maes A, et al. Clinical value of [(18)F]fluoro-deoxyglucose positron emission tomography for patients with fever of unknown origin. Clin Infect Dis. 2001;32(2):191–196. [PubMed: 11170907]

88. Seshadri N, Sonoda LI, Lever AM, Balan K. Superiority of 18F-FDG PET compared to 111In-labelled leucocyte scintigraphy in the evaluation of fever of unknown origin. J Infect. 2012;65(1):71–79. [PubMed: 22369860]

89. Takeuchi M, Dahabreh IJ, Nihashi T, Iwata M, Varghese GM, Terasawa T. Nuclear Imaging for Classic Fever of Unknown Origin: Meta-Analysis. J Nucl Med. 2016;57(12):1913–1919. [PubMed: 27339873]

90. Kagna O, Srour S, Melamed E, Militianu D, Keidar Z. FDG PET/CT imaging in the diagnosis of osteomyelitis in the diabetic foot. Eur J Nucl Med Mol Imaging. 2012;39(10):1545–1550. [PubMed: 22801731]

91. Nawaz A, Torigian DA, Siegelman ES, Basu S, Chryssikos T, Alavi A. Diagnostic performance of FDG-PET, MRI, and plain film radiography (PFR) for the diagnosis of osteomyelitis in the diabetic foot. Mol Imaging Biol. 2010;12(3):335–342. [PubMed: 19816744]

92. Schwegler B, Stumpe KD, Weishaupt D, et al. Unsuspected osteomyelitis is frequent in persistent diabetic foot ulcer and better diagnosed by MRI than by 18F-FDG PET or 99mTc-MOAB. J Intern Med. 2008;263(1):99–106. [PubMed: 18036160]

93. Basu S, Chryssikos T, Houseni M, et al. Potential role of FDG PET in the setting of diabetic neuro-osteoarthropathy: can it differentiate uncomplicated Charcot's neuroarthropathy from osteomyelitis and soft-tissue infection? Nucl Med Commun. 2007;28(6):465–472.

94. Keidar Z, Militianu D, Melamed E, Bar-Shalom R, Israel O. The diabetic foot: initial experience with 18F-FDG PET/CT. J Nucl Med. 2005;46(3):444–449. [PubMed: 15750157]

95. Zhuang H, Duarte PS, Pourdehand M, Shnier D, Alavi A. Exclusion of chronic osteomyelitis with F-18 fluorodeoxyglucose positron emission tomographic imaging. Clin Nucl Med. 2000;25(4):281–284. [PubMed: 10750968]

96. Kalicke T, Schmitz A, Risse JH, et al. Fluorine-18 fluorodeoxyglucose PET in infectious bone diseases: results of histologically confirmed cases. Eur J Nucl Med. 2000;27(5):524–528. [PubMed: 10853807]

97. Gholamrezanezhad A, Basques K, Batouli A, Matcuk G, Alavi A, Jadvar H. Clinical Nononcologic Applications of PET/CT and PET/MRI in Musculoskeletal, Orthopedic, and Rheumatologic Imaging. AJR Am J Roentgenol. 2018;210(6):W245–W263. [PubMed: 29787313]

98. Diaz LA Jr., Foss CA, Thornton K, et al. Imaging of musculoskeletal bacterial infections by [124I]FIAU-PET/CT. PLoS One. 2007;2(10):e1007. [PubMed: 17925855]

99. Dumarey N Imaging with FDG labeled leukocytes: is it clinically useful? Q J Nucl Med Mol Imaging. 2009;53(1):89–94. [PubMed: 19182732]

100. Dumarey N, Egrise D, Blocklet D, et al. Imaging infection with 18F-FDG-labeled leukocyte PET/CT: initial experience in 21 patients. J Nucl Med. 2006;47(4):625–632. [PubMed: 16595496]

101. Burge R, Dawson-Hughes B, Solomon DH, Wong JB, King A, Tosteson A. Incidence and economic burden of osteoporosis-related fractures in the United States, 2005–2025. J Bone Miner Res. 2007;22(3):465–475. [PubMed: 17144789]

102. Brauer CA, Coca-Perraillon M, Cutler DM, Rosen AB. Incidence and mortality of hip fractures in the United States. JAMA. 2009;302(14):1573–1579. [PubMed: 19826027]

103. Leibson CL, Tosteson AN, Gabriel SE, Ransom JE, Melton LJ. Mortality, disability, and nursing home use for persons with and without hip fracture: a population-based study. J Am Geriatr Soc. 2002;50(10):1644–1650. [PubMed: 12366617]

104. Keene GS, Parker MJ, Pryor GA. Mortality and morbidity after hip fractures. BMJ. 1993;307(6914):1248–1250. [PubMed: 8166806]

105. de Bakker CMJ, Tseng WJ, Li Y, Zhao H, Liu XS. Clinical Evaluation of Bone Strength and Fracture Risk. Curr Osteoporos Rep. 2017;15(1):32–42. [PubMed: 28185216]

106. Messina C, Maffi G, Vitale JA, Ulivieri FM, Guglielmi G, Sconfienza LM. Diagnostic imaging of osteoporosis and sarcopenia: a narrative review. Quant Imaging Med Surg. 2018;8(1):86–99. [PubMed: 29541625]

107. Assessment of fracture risk and its application to screening for postmenopausal osteoporosis. Report of a WHO Study Group. World Health Organ Tech Rep Ser. 1994;843:1–129. [PubMed: 7941614]

108. Kinoshita H, Tamaki T, Hashimoto T, Kasagi F. Factors influencing lumbar spine bone mineral density assessment by dual-energy X-ray absorptiometry: comparison with lumbar spinal radiogram. J Orthop Sci. 1998;3(1):3–9. [PubMed: 9654549]
109. Wainwright SA, Marshall LM, Ensrud KE, et al. Hip fracture in women without osteoporosis. J Clin Endocrinol Metab. 2005;90(5):2787–2793. [PubMed: 15728213]
110. Rajapakse CS, Chang G. Micro-Finite Element Analysis of the Proximal Femur on the Basis of High-Resolution Magnetic Resonance Images. Curr Osteoporos Rep. 2018;16(6):657–664. [PubMed: 30232586]
111. Wehrli FW. Structural and functional assessment of trabecular and cortical bone by micro magnetic resonance imaging. JMagn Reson Imaging. 2007;25(2):390–409. [PubMed: 17260403]
112. Keaveny TM, McClung MR, Genant HK, et al. Femoral and vertebral strength improvements in postmenopausal women with osteoporosis treated with denosumab. J Bone Miner Res. 2014;29(1):158–165. [PubMed: 23794225]
113. Nishiyama KK, Ito M, Harada A, Boyd SK. Classification of women with and without hip fracture based on quantitative computed tomography and finite element analysis. Osteoporos Int. 2014;25(2):619–626. [PubMed: 23948875]
114. Keyak JH, Sigurdsson S, Karlsdottir GS, et al. Effect of finite element model loading condition on fracture risk assessment in men and women: the AGES-Reykjavik study. Bone. 2013;57(1):18–29. [PubMed: 23907032]
115. Austin AG, Raynor WY, Reilly CC, et al. Evolving Role of MR Imaging and PET in Assessing Osteoporosis. PET Clin. 2019;14(1):31–41. [PubMed: 30420220]
116. Reilly CC, Raynor WY, Hong AL, et al. Diagnosis and Monitoring of Osteoporosis With (18)F-Sodium Fluoride PET: An Unavoidable Path for the Foreseeable Future. Semin Nucl Med. 2018;48(6):535–540. [PubMed: 30322479]
117. Jadvar H, Desai B, Conti PS. Sodium 18F-fluoride PET/CT of bone, joint, and other disorders. Semin Nucl Med. 2015;45(1):58–65. [PubMed: 25475379]
118. Costeas A, Woodard HQ, Laughlin JS. Depletion of 18F from blood flowing through bone. J Nucl Med. 1970;11(1):43–45. [PubMed: 5409579]
119. Blake GM, Siddique M, Frost ML, Moore AE, Fogelman I. Imaging of site specific bone turnover in osteoporosis using positron emission tomography. Curr Osteoporos Rep. 2014;12(4):475–485. [PubMed: 25168931]
120. Rhodes S, Batzdorf A, Sorci O, et al. Assessment of femoral neck bone metabolism using (18)F-sodium fluoride PET/CT imaging. Bone. 2020;136:115351. [PubMed: 32276154]
121. Frost ML, Fogelman I, Blake GM, Marsden PK, Cook G, Jr. Dissociation between global markers of bone formation and direct measurement of spinal bone formation in osteoporosis. J Bone Miner Res. 2004;19(11):1797–1804. [PubMed: 15476579]
122. Uchida K, Nakajima H, Miyazaki T, et al. Effects of alendronate on bone metabolism in glucocorticoid-induced osteoporosis measured by 18F-fluoride PET: a prospective study. J Nucl Med. 2009;50(11):1808–1814. [PubMed: 19837766]
123. Izadyar S, Gholamrezanezhad A. Bone scintigraphy elucidates different metabolic stages of melorheostosis. Pan Afr Med J. 2012;11:21. [PubMed: 22514755]
124. Installe J, Nzeusseu A, Bol A, Depresseux G, Devogelaer JP, Lonneux M. (18)F-fluoride PET for monitoring therapeutic response in Paget's disease of bone. J Nucl Med. 2005;46(10):1650–1658. [PubMed: 16204715]
125. Frost ML, Cook GJ, Blake GM, Marsden PK, Benatar NA, Fogelman I. A prospective study of risedronate on regional bone metabolism and blood flow at the lumbar spine measured by 18F-fluoride positron emission tomography. J Bone Miner Res. 2003;18(12):2215–2222. [PubMed: 14672357]
126. Frost ML, Siddique M, Blake GM, et al. Regional bone metabolism at the lumbar spine and hip following discontinuation of alendronate and risedronate treatment in postmenopausal women. Osteoporos Int. 2012;23(8):2107–2116. [PubMed: 21983795]
127. Frost ML, Siddique M, Blake GM, et al. Differential effects of teriparatide on regional bone formation using (18)F-fluoride positron emission tomography. J Bone Miner Res. 2011;26(5):1002–1011. [PubMed: 21542003]

128. Lundblad H, Karlsson-Thur C, Maguire GQ Jr., et al. Can Spatiotemporal Fluoride ((18)F(−)) Uptake be Used to Assess Bone Formation in the Tibia? A Longitudinal Study Using PET/CT. Clin Orthop Relat Res. 2017;475(5):1486–1498. [PubMed: 28150226]
129. Win AZ, Aparici CM. Normal SUV values measured from NaF18-PET/CT bone scan studies. PLoS One. 2014;9(9):e108429. [PubMed: 25254490]
130. Rebuzzi M, Vinicola V, Taggi F, Sabatini U, Wehrli FW, Capuani S. Potential diagnostic role of the MRI-derived internal magnetic field gradient in calcaneus cancellous bone for evaluating postmenopausal osteoporosis at 3T. Bone. 2013;57(1):155–163. [PubMed: 23899635]
131. Link TM, Majumdar S, Augat P, et al. In vivo high resolution MRI of the calcaneus: differences in trabecular structure in osteoporosis patients. JBone Miner Res. 1998;13(7):1175–1182. [PubMed: 9661082]
132. Zirakchian Zadeh M, Ostergaard B, Raynor WY, et al. Comparison of (18)F-sodium fluoride uptake in the whole bone, pelvis, and femoral neck of multiple myeloma patients before and after high-dose therapy and conventional-dose chemotherapy. Eur J Nucl Med Mol Imaging. 2020.
133. Rajapakse CS, Phillips EA, Sun W, et al. Vertebral deformities and fractures are associated with MRI and pQCT measures obtained at the distal tibia and radius of postmenopausal women. Osteoporos Int. 2014;25(3):973–982. [PubMed: 24221453]
134. Blake GM, Puri T, Siddique M, Frost ML, Moore AEB, Fogelman I. Site specific measurements of bone formation using [(18)F] sodium fluoride PET/CT. Quant Imaging Med Surg. 2018;8(1):47–59. [PubMed: 29541623]
135. Jones HR Jr, Burns T, Aminoff MJ, Pomeroy S. The Netter Collection of Medical Illustrations: Nervous System, Volume 7, Part II-Spinal Cord and Peripheral Motor and Sensory Systems E-Book. Elsevier Health Sciences; 2013.
136. Tieland M, Trouwborst I, Clark BC. Skeletal muscle performance and ageing. J Cachexia Sarcopenia Muscle. 2018;9(1):3–19. [PubMed: 29151281]
137. Otto EB, Dworzecki T. The role of skeletal muscle in the regulation of glucose homeostasis. Endokrynologia, diabetologia i choroby przemiany materii wieku rozwojowego: organ Polskiego Towarzystwa Endokrynologow Dzieciecych. 2003;9(2):93–97.
138. Reid KF, Fielding RA. Skeletal muscle power: a critical determinant of physical functioning in older adults. Exerc Sport Sci Rev. 2012;40(1):4–12. [PubMed: 22016147]
139. Stump CS, Henriksen EJ, Wei Y, Sowers JR. The metabolic syndrome: role of skeletal muscle metabolism. Ann Med. 2006;38(6):389–402. [PubMed: 17008303]
140. Boutin RD, Yao L, Canter RJ, Lenchik L. Sarcopenia: Current Concepts and Imaging Implications. AJR Am JRoentgenol. 2015;205(3):W255–266. [PubMed: 26102307]
141. Morley JE, Thomas DR, Wilson MM. Cachexia: pathophysiology and clinical relevance. Am J Clin Nutr. 2006;83(4):735–743. [PubMed: 16600922]
142. Cawthon PM, Lui LY, Taylor BC, et al. Clinical Definitions of Sarcopenia and Risk of Hospitalization in Community-Dwelling Older Men: The Osteoporotic Fractures in Men Study. J Gerontol A Biol Sci Med Sci. 2017;72(10):1383–1389. [PubMed: 28329087]
143. Steffl M, Sima J, Shiells K, Holmerova I. The increase in health care costs associated with muscle weakness in older people without long-term illnesses in the Czech Republic: results from the Survey of Health, Ageing and Retirement in Europe (SHARE). Clinical Interventions in Aging. 2017;12:2003. [PubMed: 29225462]
144. Anker SD, Morley JE, von Haehling S. Welcome to the ICD-10 code for sarcopenia. J Cachexia Sarcopenia Muscle. 2016;7(5):512–514. [PubMed: 27891296]
145. Cruz-Jentoft AJ, Bahat G, Bauer J, et al. Sarcopenia: revised European consensus on definition and diagnosis. Age and ageing. 2019;48(1):16–31. [PubMed: 30312372]
146. Albano D, Messina C, Vitale J, Sconfienza LM. Imaging of sarcopenia: old evidence and new insights. Eur Radiol. 2020;30(4):2199–2208.
147. Lenchik L, Boutin RD. Sarcopenia: beyond muscle atrophy and into the new frontiers of opportunistic imaging, precision medicine, and machine learning. Paper presented at: Seminars in musculoskeletal radiology 2018.
148. Raitakari M, Nuutila P, Ruotsalainen U, et al. Evidence for dissociation of insulin stimulation of blood flow and glucose uptake in human skeletal muscle: studies using [15O] H2O,[18F]

fluoro-2-deoxy-D-glucose, and positron emission tomography. Diabetes. 1996;45(11):1471–1477. [PubMed: 8866549]

149. Zhou C, Foster B, Hagge R, et al. Opportunistic body composition evaluation in patients with esophageal adenocarcinoma: association of survival with 18 F-FDG PET/CT muscle metrics. Annals of Nuclear Medicine. 2020;34(3): 174–181. [PubMed: 31823231]
150. Kothekar E, Raynor WY, Al-Zaghal A, Jonnakuti VS, Werner TJ, Alavi A. Evolving Role of PET/CT-MRI in Assessing Muscle Disorders. PET Clin. 2019;14(1):71–79. [PubMed: 30420223]
151. Rudroff T, Kindred JH, Kalliokoski KK. [18F]-FDG positron emission tomography—an established clinical tool opening a new window into exercise physiology. Journal of Applied Physiology. 2015;118(10):1181–1190. [PubMed: 25767034]
152. Rudroff T, Weissman JA, Bucci M, et al. Positron emission tomography detects greater blood flow and less blood flow heterogeneity in the exercising skeletal muscles of old compared with young men during fatiguing contractions. JPhysiol. 2014;592(2):337–349. [PubMed: 24247981]
153. Foster B, Boutin RD, Lenchik L, et al. Skeletal Muscle Metrics on Clinical (18)F-FDG PET/CT Predict Health Outcomes in Patients with Sarcoma. J Nat Sci. 2018;4(5).
154. Ruotsalainen U, Raitakari M, Nuutila P, et al. Quantitative blood flow measurement of skeletal muscle using oxygen-15-water and PET. Journal of Nuclear Medicine. 1997;38(2):314. [PubMed: 9025761]
155. Nuutila P, Raitakari M, Laine H, et al. Role of blood flow in regulating insulin-stimulated glucose uptake in humans. Studies using bradykinin,[15O] water, and [18F] fluoro-deoxyglucose and positron emission tomography. The Journal of clinical investigation. 1996;97(7):1741–1747. [PubMed: 8601640]
156. Clyne CA, Jones T, Moss S, Ensell J. The use of radioactive oxygen to study muscle function in peripheral vascular disease. Surgery, gynecology & obstetrics. 1979;149(2):225–228.
157. Fischman AJ, Yu YM, Livni E, et al. Muscle protein synthesis by positron-emission tomography with L-[methyl-11C]methionine in adult humans. Proc Natl Acad Sci U S A. 1998;95(22):12793–12798. [PubMed: 9788993]
158. Peltoniemi P, Lönnroth P, Laine H, et al. Lumped constant for [18F] fluorodeoxyglucose in skeletal muscles of obese and nonobese humans. American Journal of Physiology-Endocrinology And Metabolism. 2000;279(5):E1122–E1130. [PubMed: 11052968]
159. Nuutila P, Koivisto VA, Knuuti J, et al. Glucose-free fatty acid cycle operates in human heart and skeletal muscle in vivo. J Clin Invest. 1992;89(6):1767–1774. [PubMed: 1601987]
160. Mossberg KA, Rowe RW, Tewson TJ, Taegtmeyer H. Rabbit hindlimb glucose uptake assessed with positron-emitting fluorodeoxyglucose. JAppl Physiol (1985). 1989;67(4):1569–1577. [PubMed: 2676956]
161. Chou TH, Stacy MR. Clinical Applications for Radiotracer Imaging of Lower Extremity Peripheral Arterial Disease and Critical Limb Ischemia. Mol Imaging Biol. 2020;22(2):245–255.
162. Barrington S, Blower P, Cook G. New horizons in multimodality molecular imaging and novel radiotracers. Clin Med (Lond). 2017;17(5):444–448. [PubMed: 28974596]
163. Wu C, Yue X, Lang L, et al. Longitudinal PET imaging of muscular inflammation using 18F-DPA-714 and 18F-Alfatide II and differentiation with tumors. Theranostics. 2014;4(5):546. [PubMed: 24672585]
164. Lu Y, Karagounis LG, Ng TP, et al. Systemic and Metabolic Signature of Sarcopenia in Community-Dwelling Older Adults. J Gerontol A Biol Sci Med Sci. 2020;75(2):309–317. [PubMed: 30624690]
165. Baracos VE. Psoas as a sentinel muscle for sarcopenia: a flawed premise. Journal of Cachexia, Sarcopenia and Muscle. 2017;8(4):527–528.
166. Rutten IJ, Ubachs J, Kruitwagen RF, Beets-Tan RG, Olde Damink SW, Van Gorp T. Psoas muscle area is not representative of total skeletal muscle area in the assessment of sarcopenia in ovarian cancer. Journal of Cachexia, Sarcopenia and Muscle. 2017;8(4):630–638.
167. Ng JM, Bertoldo A, Minhas DS, et al. Dynamic PET imaging reveals heterogeneity of skeletal muscle insulin resistance. J Clin Endocrinol Metab. 2014;99(1):E102–106. [PubMed: 24170108]

168. Kalliokoski KK, Kemppainen J, Larmola K, et al. Muscle blood flow and flow heterogeneity during exercise studied with positron emission tomography in humans. Eur J Appl Physiol. 2000;83(4 −5):395–401. [PubMed: 11138581]

169. Batouli A, Braun J, Singh K, Gholamrezanezhad A, Casagranda BU, Alavi A. Diagnosis of non-osseous spinal metastatic disease: the role of PET/CT and PET/MRI. J Neurooncol. 2018;138(2):221–230. [PubMed: 29484521]

170. Behzadi AH, Raza SI, Carrino JA, et al. Applications of PET/CT and PET/MR Imaging in Primary Bone Malignancies. PET Clin. 2018;13(4):623–634. [PubMed: 30219192]

171. Cleary MX, Fayad LM, Ahlawat S. Popliteal lymph nodes in patients with osteosarcoma: are they metastatic? Skeletal Radiol. 2020.

172. Erfanian Y, Grueneisen J, Kirchner J, et al. Integrated 18F-FDG PET/MRI compared to MRI alone for identification of local recurrences of soft tissue sarcomas: a comparison trial. Eur J Nucl Med Mol Imaging. 2017;44(11):1823–1831. [PubMed: 28567495]

173. Assadi M, Velez E, Najafi MH, Matcuk G, Gholamrezanezhad A. PET Imaging of Peripheral Nerve Tumors. PET Clin. 2019;14(1):81–89. [PubMed: 30420224]

174. Lee I, Byun BH, Lim I, et al. Early response monitoring of neoadjuvant chemotherapy using [(18)F]FDG PET can predict the clinical outcome of extremity osteosarcoma. EJNMMIRes. 2020;10(1):1.

175. Sheen H, Kim W, Byun BH, et al. Metastasis risk prediction model in osteosarcoma using metabolic imaging phenotypes: A multivariable radiomics model. PLoS One. 2019;14(11):e0225242. [PubMed: 31765423]

176. Jeong SY, Kim W, Byun BH, et al. Prediction of Chemotherapy Response of Osteosarcoma Using Baseline (18)F-FDG Textural Features Machine Learning Approaches with PCA. Contrast Media Mol Imaging. 2019;2019:3515080. [PubMed: 31427908]

177. Bosma SE, Vriens D, Gelderblom H, van de Sande MAJ, Dijkstra PDS, Bloem JL. (18)F-FDG PET-CT versus MRI for detection of skeletal metastasis in Ewing sarcoma. Skeletal Radiol. 2019;48(11):1735–1746. [PubMed: 31016339]

178. Gholamrezanezhad A, Guermazi A, Salavati A, Alavi A. PET-Computed Tomography and PET-MR Imaging and Their Applications in the Twenty-First Century. PET Clin. 2019;14(1):xv–xvii. [PubMed: 30420226]

179. Gholamrezanejhad A, Mirpour S, Mariani G. Future of nuclear medicine: SPECT versus PET. J Nucl Med. 2009;50(7):16N–18N.

180. Batouli A, Gholamrezanezhad A, Petrov D, Rudkin S, Matcuk G, Jadvar H. Management of Primary Osseous Spinal Tumors with PET. PET Clin. 2019;14(1):91–101. [PubMed: 30420225]

181. Khalatbari H, Parisi MT, Kwatra N, Harrison DJ, Shulkin BL. Pediatric Musculoskeletal Imaging: The Indications for and Applications of PET/Computed Tomography. PET Clin. 2019;14(1):145–174. [PubMed: 30420216]

182. Katal S, Gholamrezanezhad A, Kessler M, Olyaei M, Jadvar H. PET in the Diagnostic Management of Soft Tissue Sarcomas of Musculoskeletal Origin. PET Clin. 2018;13(4):609–621. [PubMed: 30219191]

183. Raynor WY, Al-Zaghal A, Zadeh MZ, Seraj SM, Alavi A. Metastatic Seeding Attacks Bone Marrow, Not Bone: Rectifying Ongoing Misconceptions. PET Clin. 2019;14(1):135–144. [PubMed: 30420215]

184. Kothekar E, Yellanki D, Borja AJ, et al. 18F-FDG-PET/CT in measuring volume and global metabolic activity of thigh muscles: a novel CT-based tissue segmentation methodology. Nucl Med Commun. 2020;41(2):162–168.

Key Points (3-5 bulleted sentences indicating the main takeaways/defining elements of the article)

- A number of musculoskeletal disorders are systemic in nature or have systemic sequalae. Biomarkers that provide global assessment of disease activity across the entire body are urgently needed.
- Total-body PET/CT can provide anato-molecular imaging-based measures across the entire human body at reduced dose, lower scan time, and higher spatial resolution.
- Total-body Pet/CT measures can contribute towards an improved understanding of the underlying pathogenesis of musculoskeletal disorders and may provide new insights for the evaluation of and monitoring of interventions and therapy.
- Since total-body PET/CT includes images of the brain in the field of view, this approach may provide a means to detect and quantify the degree of pain that is associated with musculoskeletal disorders, potentially allowing further insight into the impact of opioids.

Synopsis

Imaging of musculoskeletal disorders, including arthritis, infection, osteoporosis, sarcopenia, and malignancies, is often limited when using conventional modalities such as radiography, CT, and MRI. As a result of recent advances in PET instrumentation, total-body PET/CT offers a longer axial field-of-view, higher geometric sensitivity, and higher spatial resolution compared to standard PET systems. This article discusses the potential applications of total-body PET/CT imaging in the assessment of musculoskeletal disorders.

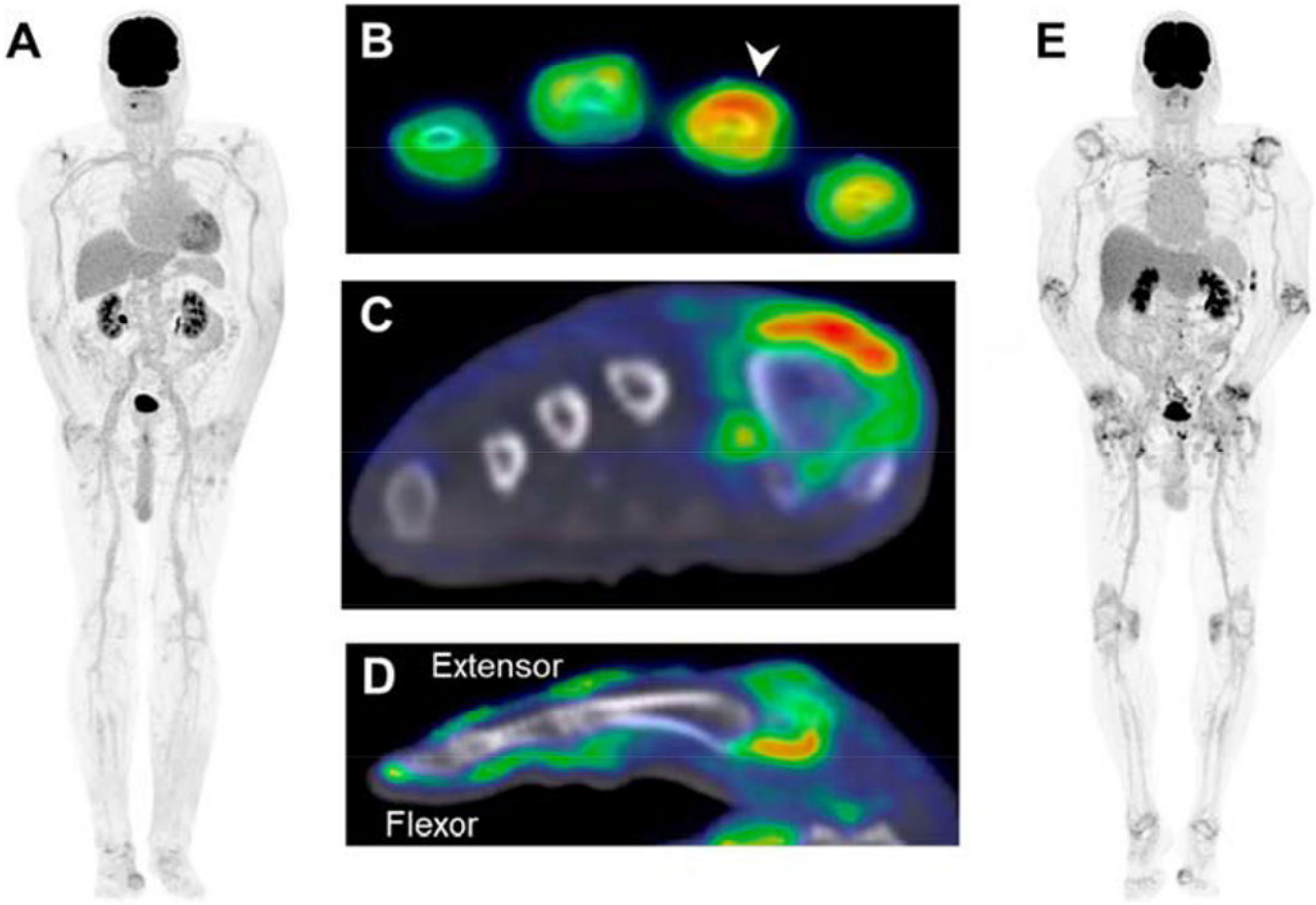

Figure 1.

TB PET in rheumatoid and psoriatic arthritis. Maximum intensity projection (MIP) from the TB PET scan of a 65-year-old man with established rheumatoid arthritis (A). Images of the subject in (A) showing classic ring-like patterns of radiotracer uptake consistent with synovitis in the joints of the hand (B), and foot (C). Extensor and flexor tenosynovitis and enthesitis in the right second digit of a 72-year-old man with established psoriatic arthritis (D), also shown in the MIP of the TB PET scan (E). These images were acquired on the uEXPLORER PET/CT scanner at the University of California Davis, with an injected dose of about 74 MBq. Images show static scans conducted over 20 min, starting at 40 min post-radiotracer injection.

Courtesy of Y. Abdelhafez, MD, University of California Davis

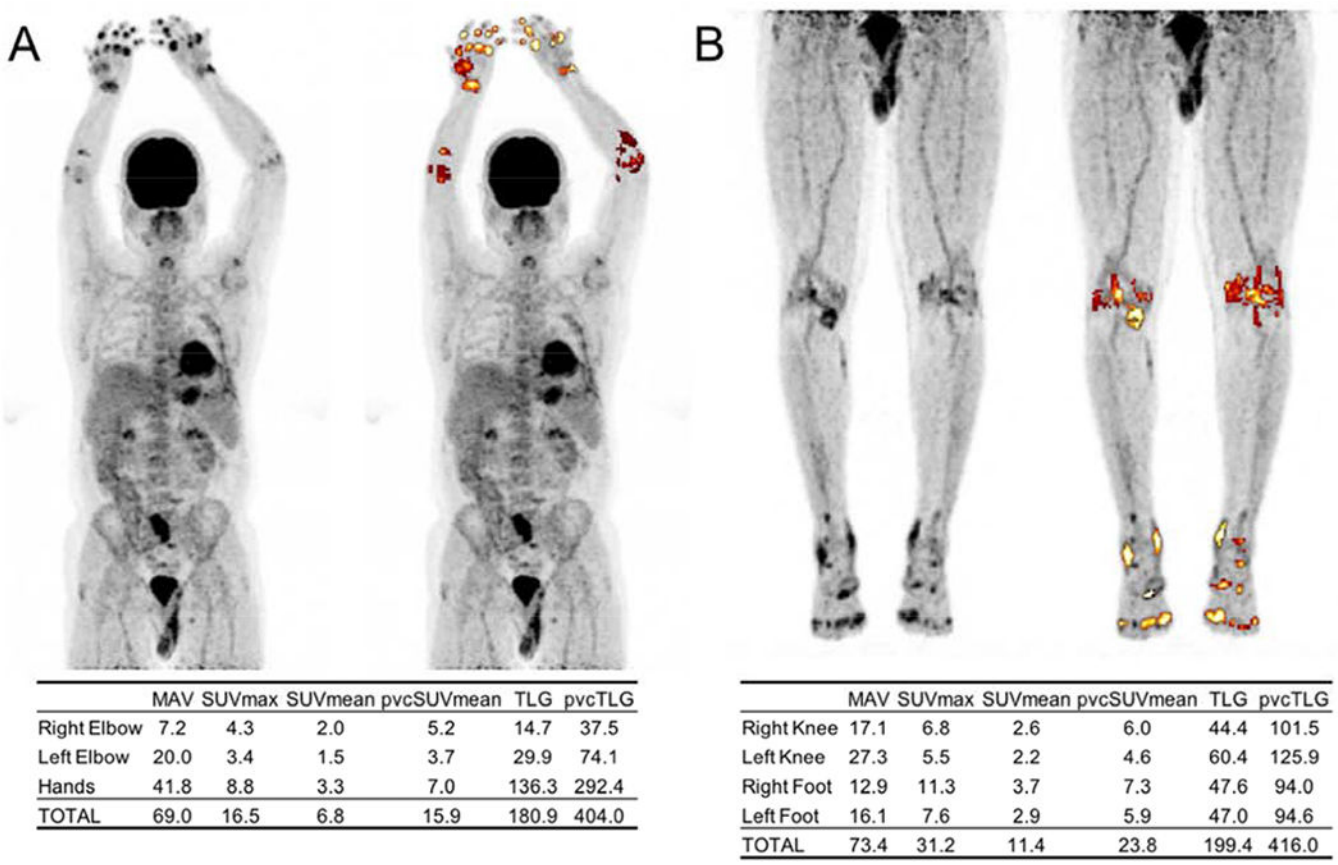

	MAV	SUVmax	SUVmean	pvcSUVmean	TLG	pvcTLG
Right Elbow	7.2	4.3	2.0	5.2	14.7	37.5
Left Elbow	20.0	3.4	1.5	3.7	29.9	74.1
Hands	41.8	8.8	3.3	7.0	136.3	292.4
TOTAL	69.0	16.5	6.8	15.9	180.9	404.0

	MAV	SUVmax	SUVmean	pvcSUVmean	TLG	pvcTLG
Right Knee	17.1	6.8	2.6	6.0	44.4	101.5
Left Knee	27.3	5.5	2.2	4.6	60.4	125.9
Right Foot	12.9	11.3	3.7	7.3	47.6	94.0
Left Foot	16.1	7.6	2.9	5.9	47.0	94.6
TOTAL	73.4	31.2	11.4	23.8	199.4	416.0

Figure 2.

FDG-PET maximum intensity projection (MIP) of a 69-year-old man with rheumatoid arthritis showing the upper body (A) and lower body (B). Synovitis was assessed by segmenting FDG-avid joints using an adaptive thresholding algorithm (ROVER software, ABX GmbH, Radeberg, Germany). Metabolically active volume (MAV), maximum standardized uptake value (SUV_{max}), mean SUV (SUV_{mean}), partial volume-corrected SUV_{mean} ($pvcSUV_{mean}$), total lesion glycolysis (TLG = MAV × SUV_{mean}), and partial volume-corrected TLG (pvcTLG = MAV × $pvcSUV_{mean}$) were calculated and summed for each segmented region. The global pvcTLG for this patient was 820.0. These analyses could be enabled at a lower radiation dose and scan time, with more comprehensive body coverage in a single scan, using TB PET/CT.

From Saboury B, Morris MA, Nikpanah M, Werner TJ, Jones EC, Alavi A. Reinventing Molecular Imaging with Total-Body PET, Part II: Clinical Applications. PET Clin. 2020;15(4):463-475. doi:10.1016/j.cpet.2020.06.013; with permission.

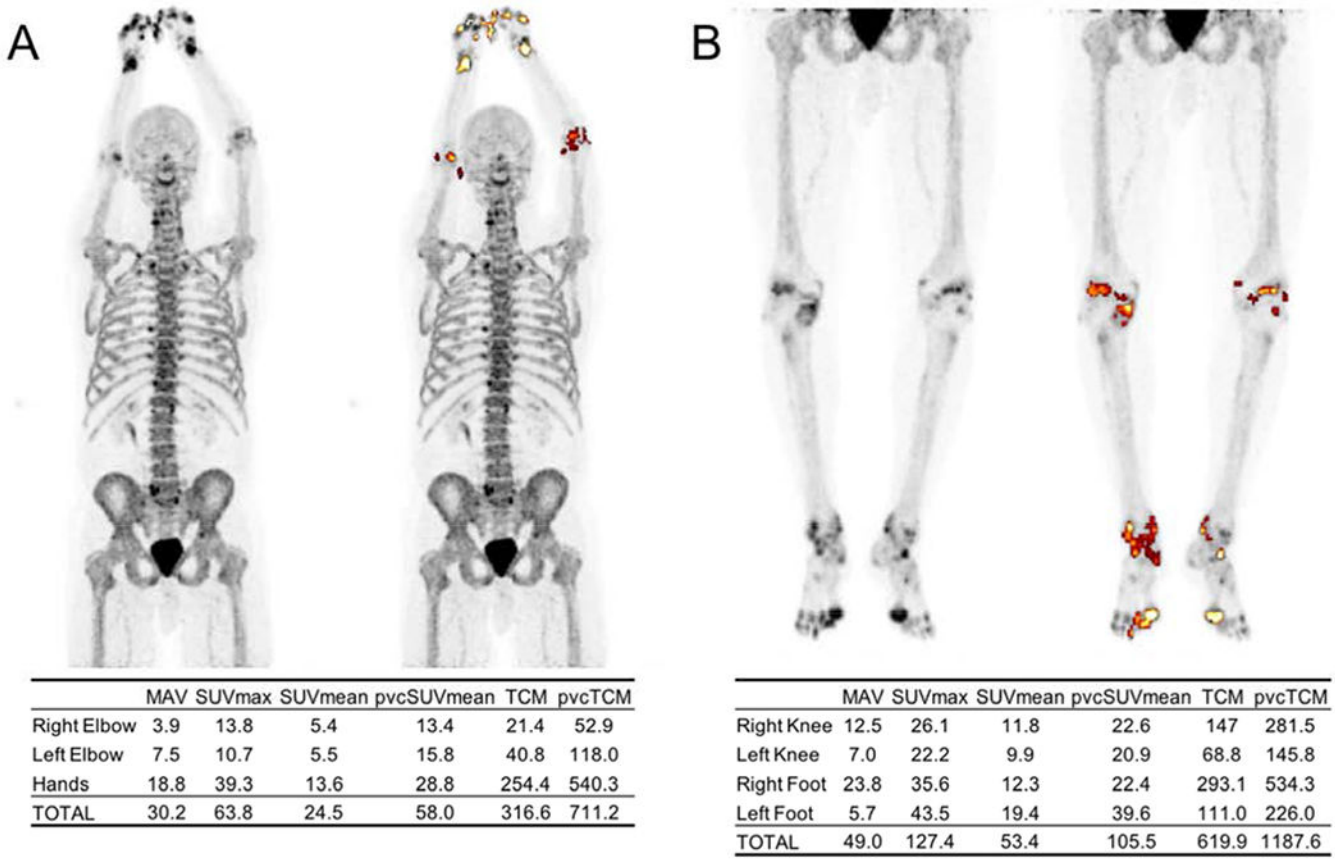

	MAV	SUVmax	SUVmean	pvcSUVmean	TCM	pvcTCM
Right Elbow	3.9	13.8	5.4	13.4	21.4	52.9
Left Elbow	7.5	10.7	5.5	15.8	40.8	118.0
Hands	18.8	39.3	13.6	28.8	254.4	540.3
TOTAL	30.2	63.8	24.5	58.0	316.6	711.2

	MAV	SUVmax	SUVmean	pvcSUVmean	TCM	pvcTCM
Right Knee	12.5	26.1	11.8	22.6	147	281.5
Left Knee	7.0	22.2	9.9	20.9	68.8	145.8
Right Foot	23.8	35.6	12.3	22.4	293.1	534.3
Left Foot	5.7	43.5	19.4	39.6	111.0	226.0
TOTAL	49.0	127.4	53.4	105.5	619.9	1187.6

Figure 3.

NaF-PET maximum intensity projection (MIP) of the same rheumatoid arthritis patient as Figure 2 showing the upper body (A) and lower body (B). ROVER software was used to segment focal areas of high bone formation in the joints. Metabolically active volume (MAV), maximum standardized uptake value (SUV_{max}), mean SUV (SUV_{mean}), partial volume-corrected SUV_{mean} ($pvcSUV_{mean}$), total calcium metabolism (TCM = MAV × SUV_{mean}), and partial volume-corrected TCM (pvcTCM = MAV × $pvcSUV_{mean}$) were calculated and summed for each segmented region. The global pvcTCM for this patient was 1898.8.

From Saboury B, Morris MA, Nikpanah M, Werner TJ, Jones EC, Alavi A. Reinventing Molecular Imaging with Total-Body PET, Part II: Clinical Applications. *PET Clin.* 2020;15(4):463-475. doi:10.1016/j.cpet.2020.06.013

Figure 4.

NaF-PET maximum intensity projection (MIP) of a 72-year-old man showing tracer uptake in the joints before (A) and after (B) PET segmentation using an adaptive thresholding algorithm (ROVER software). Volumetric and metabolic parameters were automatically calculated and summed to determine total disease activity. The global partial volume-corrected total calcium metabolism for this patient was 338.6.

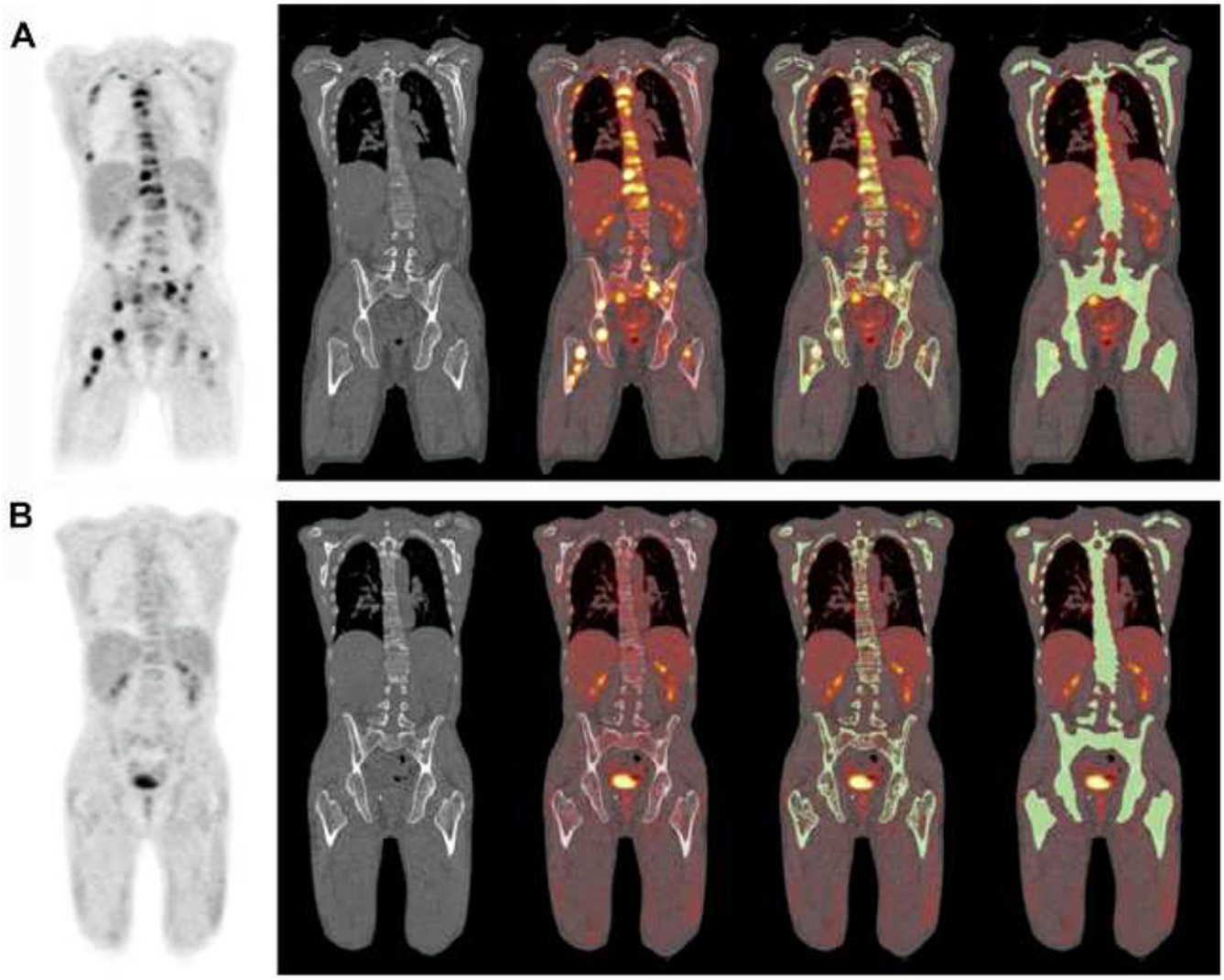

Figure 5.

Whole-body FDG-PET/CT images of a 60-year-old man with multiple myeloma. The cortical bone and bone marrow were segmented using a growing region algorithm based on Hounsfield units, followed by smoothing and closing algorithms (OsiriX software; Pixmeo SARL; Bernex, Switzerland). The global SUV_{mean}, which represents the whole bone marrow activity, before initiating treatment (A) was 2.02 and decreased to 1.10 after finishing the course of treatment (B).

(From Raynor WY, Al-Zaghal A, Zadeh MZ, Seraj SM, Alavi A. Metastatic Seeding Attacks Bone Marrow, Not Bone: Rectifying Ongoing Misconceptions. PET Clin. 2019;14(1): 135-144; with permission)

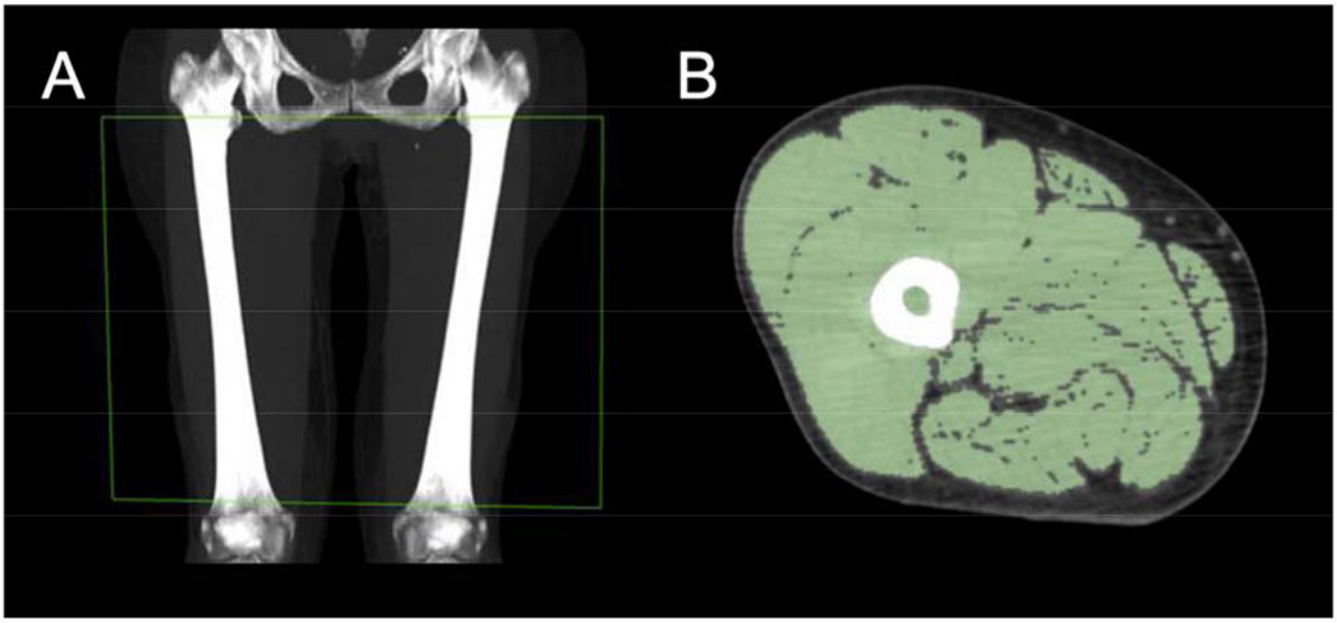

Figure 6.

Maximum intensity projection (MIP) of the CT image (A) showing a methodology used to segment muscle. Two lines (horizontal parallel green lines) corresponding to 5 cm above the intercondylar notch and 5 cm below the greater trochanter were manually delineated according to pre-determined anatomical criteria. A growing region algorithm with lower and upper thresholds of 1 and 150 Hounsfield units, respectively, was used to segment the muscle (OsiriX software) (B). Applying this methodology to 71 subjects, thigh muscle volume was found to decrease with age, and uptake of FDG uptake was found to be significantly higher on the right side compared to the left.

(From Kothekar E, Yellanki D, Borja AJ, et al. 18F-FDG-PET/CT in measuring volume and global metabolic activity of thigh muscles: a novel CT-based tissue segmentation methodology. *Nucl Med Commun*. 2020;41(2):162-168.; with permission)

Figure 7.

A 58-year-old man with toe pain was evaluated with MRI of the foot. A marrow-replacing lesion of the first distal phalanx with T_2 hyper- (A) and T_1 hypo-signal intensity (B) was identified, the tissue sampling of which was consistent with osteosarcoma. After surgical resection and several courses of chemotherapy (C), the patient returned for restaging with whole-body FDG-PET/CT. A hypermetabolic right ankle (Kager fat pad, D, E) and inguinal

lymph nodes (D) with respective SUV_{max} of 4.4 and 10.4 were identified, in keeping with metastatic lymphadenopathy.